The Florida Catastrophic Storm Risk Management Center

White Paper

Release Date:
January 2010

Improved Analysis and Understanding of the Meteorology Underlying Various Components of the Hurricane Risk Problem

THE FLORIDA STATE UNIVERSITY
COLLEGE OF BUSINESS
The Florida Catastrophic Storm Risk Management Center

IMPROVED ANALYSIS AND UNDERSTANDING OF THE METEOROLOGY UNDERLYING THE VARIOUS COMPONENTS OF THE HURRICANE RISK PROBLEM

By

Professors Robert E. Hart, Henry Fuelberg, and Paul Reasor
Graduate Students Andrew Murray, Matthew Onderlinde, Elizabeth Minter

Department of Meteorology
Florida State University
Tallahassee. FL 32306-4520
(850) 644-6205 (Voice)
(850-644-9642) (FAX)
rhart@fsu.edu
fuelberg@met.fsu.edu
reasor@met.fsu.edu
amurray@met.fsu.edu
mjonder@met.fsu.edu
eminter@met.fsu.edu

A Project Completed for the Florida Catastrophic Storm Risk Management Center
Florida State University

January 2010

TABLE OF CONTENTS

Final report for Hart SubProject…….3

Final report for Fuelberg SubProject……..19

Final report for Reasor SubProject…….31

FINAL REPORT OF THE SUBPROJECT ENTITLED:

"Statistical analysis of 1988-2008 Reconnaissance vortex messages to improve the risk climatology of hurricane intensity change and its predictability"

ROBERT HART, PI
ANDREW MURRAY, GRADUATE STUDENT

1. Background and Introduction

Until the Atlantic hurricane seasons of 2007 to the present, tropical cyclone (TC) activity in the Atlantic basin had been relatively high over the last two decades. Rappaport et al. (2009) make note of the fact that this activity included the busiest season ever recorded (2005, with 28 TCs); one of the deadliest TCs (Mitch 1998); as well as the deadliest TC to strike the U.S. in nearly a century and the most costly TC in U.S. history (Katrina 2005). Many of these problems were exacerbated by rather extreme forecast challenges in which available guidance as well as operational forecasts fell short of the accuracy desired. Figure 1.1 shows the annual average track errors for the official forecasts (OFCL) from the National Hurricane Center (NHC) with least-squares trendlines superimposed. It is apparent that the average error has been at least halved for almost every forecast length, with 96-120 h forecasts being the only exceptions. These improvements are substantial, with these improvements in track forecasts due largely to advances in Numerical Weather Prediction (NWP) guidance (Rappaport et al. 2009).

Figure 1.2 offers a sobering picture of the state of TC intensity forecasting, however. NHC annual average intensity forecast errors are shown for the period 1990-2008, again with least-squares trendlines superimposed. Given that NHC OFCL forecasts are issued to the nearest 5 knots (kt), it is difficult to discern a statistically significant improvement in the average error of NHC OFCL intensity forecasts. This relatively small change in forecast skill is startling, considering that much prior research has indicated that intensity forecasts should be closely tied to track forecasts. The apparent resultant dichotomy seems to indicate that the model improvements that have produced more accurate track forecasts may not translate to better intensity forecasts. This research sought to use inner-core measurements of TCs rather than largescale environmental factors to improve the state of TC intensity

forecasting with an underlying goal of helping to save lives and reduce the cost of damages incurred from TCs.

Much research has been devoted to improving TC intensity change forecasts during the last few decades. However, as noted earlier, improvements in intensity forecasting still lag well behind those of track forecasting. In fact, average 24-h NHC OFCL forecast errors appear to have remained virtually constant over the last 20 years (Figure 1.2), demonstrating the need for improved intensity forecasts. The research presented here expands on the preliminary research performed by Piech (2007). An updated VDM climatology is developed to encompass the time period from 1991-2008, and a simple climatological forecasting tool based on initial eye diameter and maximum sustained surface wind speed is presented. Finally, a stepwise multiple linear regression technique (ASPIRE) is utilized to produce SHIPS-style forecasts from 12 h to 48 hr for well-developed (possessing a defined eye) TCs in the Atlantic basin. The resulting forecast tool was then applied to a fully independent dataset in 2009.

This final report is divided into two sections after this introduction. The first is a review of the scientific questions to be addressed by the research, as detailed in the original proposal. The second section details the results on those questions.

2. Scientific Questions to be Addressed

Results of the research fall into three categories: Production of the climatology dataset for hurricane structure, production and validation of a forecast tool for intensity change, and publication of the research results. The climatological dataset will be made available to the broader scientific community for their own use through web servers at FSU Meteorology. Submission for publication is anticipated in Summer 2010, as a draft of the manuscript is currently in production.

The following scientific questions were addressed by the proposed research, as also noted in the original proposal:

1. What is the distribution of eye structure for all Atlantic tropical cyclones?
2. What is the climatological intensity change in the hours following the existence in 1)?
3. When 2) is used as a forecast, does the resulting performance surpass that of persistence and SHIPS?
4. What insight do the chosen predictors give for the science of short-term intensity change?

3. Results of Subproject

Mr. Andrew Murray, then an M.S. candidate at FSU, was been funded for his thesis research on this component of the grant, with additional funding provided by a NASA grant. His research findings are discussed below, but can be found in full from his M.S. thesis document soon available online from FSU. A PDF of his thesis is available from the PI until that time. He defended his thesis in November 2009, and subsequently began a teaching career at Univ. S. Alabama in January of 2010. Mr. Murray will be presenting his M.S. thesis research at both the AMS Annual Meeting in Atlanta, GA in January 2010 and at the AMS Hurricanes and Tropical Meteorology Conference in Tuscon, AZ, in May 2010.

a. Refined and expanded climatology

We have refined and extended the climatological database developed by Piech (2007) to include storms since 2005. Further, a subjective analysis of the vortex message database was replaced with the use of the ATCF f-deck database. The use of the NHC f-deck database minimizes the potential for typographical errors since that database was created by existing software at NHC, using the vortex message database as the foundation.

One drawback of the vortex message/f-deck database (which will be used interchangeably here) is that there are not routinely reliable measures of observed peak surface wind. While observed or extrapolated core surface pressure is reported reliably, a peak wind speed largely depends on the success of releasing a dropsonde directly into an eyewall (which slopes) from flight level, or reducing peak flight level winds to the surface. Given this inhomogeneity, we added to the vortex message database the NHC advisory (a-deck) sustained wind speed that precedes the vortex message report. This permits a reliable sustained peak wind speed to be associated with every vortex message report, and enables forecast verification given surface pressure is not a forecast variable by statistical (e.g. SHIPS; DeMaria and Kaplan 1994, 1999) and NHC forecasts.

The resulting climatology of existence as a function of wind speed and eye size is given in Figure 1.1, demonstrating a pattern consistent with the Piech (2007) climatology as a function of surface pressure and eye size. This consistency provides confidence that the use of a precursor advisory wind speed as a measure of intensity to collocate with the vortex message report is valid. The resulting forecast performance (discussed later) further validates this relationship.

By using the advisory wind speed as the intensity measures, we can now calculate a wind speed intensity change by examining the change in sustained advisory wind speed between the two consecutive 6hrly advisory reports (one that precedes the vortex message and one that follows). The

resulting future intensity change as a function of initial intensity and eye size is given in Figure 1.4. On average, at intensities less (greater) than 95kt, there is intensification (weakening) at all eye sizes. This argues that fundamentally, 95kt represents a mean transition intensity in the evolution of a hurricane that begs further examination. The standard error of this mean intensity change (not shown here but shown in the Murray M.S. thesis document) argues that there is great case-to-case variability about this mean, and that use of this climatological forecast alone is unlikely to be sufficient to reliably forecast intensity change. Nonetheless, the future intensity change forecast by this diagram will be one predictor used in the stepwise regression that is performed in the next stage of the research, to be discussed next.

b. Stepwise regression

The existing benchmark for statistical hurricane intensity forecasting, SHIPS, primarily utilizes measurements or estimates of the environment of a hurricane, such as SST, shear, angular momentum import, and potential intensity. What this benchmark is missing is observational measurements of the core of the storm, which prior research and theory have shown are key to hurricane intensity change. The ongoing research seeks to incorporate these core measurements to produce a more skillful benchmark for hurricane intensity forecasting. In addition to the numerous measurements reported in each vortex message (latitude, longitude, time, eye temperature, eye dewpoint, temperature outside eye, surface pressure, eye size and type), many linear and nonlinear combinations of predictors were calculated (theta and theta-e inside and outside eye, area of eye, area of eye multiplied by the prior thermodynamic parameters, dynamic measures of inertial stability, to name a few).

All of the parameters that were selected at the final stage of the stepwise regression process are listed in Figure 1.5. Many of the predictors were chosen using existing knowledge of the Sawyer-Eliassen secondary circulation and its relationship to hurricane intensity change (Eliassen 1951; Shapiro and Willoughby 1982). For example, predictors such as the area of the eye multiplied by the potential temperature are a proxy for the strength of the mass subsidence within the eye – one measure of the storm's potential for intensification. All potential predictors distributions were examined for their normality (or lack thereof), and transformed using exponentials or logarithms as necessary to more closely approach normality. Figures 1.6 and 1.7 demonstrate the transformation of two significant predictors from highly skewed distributions to approximately normal distributions. Such transformations increase the potential predictive power of the stepwise regression by reducing the skewed distribution of the residuals following each regression step, and increasing the explained variance at each step. The Minitab software used filters the predictors at each step of the stepwise

regression to eliminate predictors that are highly covarying, and will remove previously chosen predictors should new predictors explain more variance when prior predictors are removed.

Two different sets of forecast equations are developed. The first set of equations uses all data at all initial intensities for a given forecast length. Thus, there is one equation for forecast hour 12, one equation for forecast hour 18, onward through 48hr. These forecasts are represented by the green lines in Figures 1.8-1.11. The second set of forecast equations were developed by producing running bins of 20kt size for the initial intensity. For example, the forecast equation in equation set 2 for an initial intensity of 75kt was developed using data for an initial intensity of 65kt through 85kt. This second set of equations is represented by the blue lines in Figures 1.8-1.11. For comparison, the SHIPS forecast is given in red in those same figures.

c. Out-of-sample performance of regression

It must first be noted that the measure of performance to be used for skill evaluation was the out-of-sample R-squared, also known as R-squared-predicted by the software used for the regression (Minitab). This out of sample R-squared is performed by removing one set of data points from the regression, doing the stepwise regression, and then predicting the removed verification datapoint. That process is repeated N times, and the R-squared value is reported for the out-of-sample dataset of N size. The consequence of this out-of-sample measurement is that it gives a robust estimate of the predictive skill of the regression equation (since it simulates future unknown data) and minimizes the potential for overfitting to the development dataset.

Out-of-sample R-squared performance measures are given in Figures 1.8-1.11 for 12, 24, 36, and 48hr forecasts, comparing the regression equation using all initial intensities (green lines), the regression equations using initial intensity subsets (blue lines), and the SHIPS forecasts (in red lines). Performance overall outpredicts SHIPS by a considerable margin, most notably at the highest initial intensities (category 4 or 5), which has considerable societal impact. The performance is summarized more effectively in Figure 1.12, which plots the shading of R-squared (again, out of sample) as a function of forecast length and initial intensity. What is immediately apparent is that the predictability of intensity is strongly a function of the initial intensity of the hurricane – with three minima of forecast confidence at the 60kt, 105kt, and 140kt intensities. These regimes of decreased forecast confidence likely are related to the occurrence of concentric eyewall occurrence (consistent with Piech 2007). Nonetheless, the performance overall is a marked improvement upon SHIPS and a real-time web site is being developed that implements these equations for real-time forecasting as reconnaissance reports are

received. Figure 1.11 lists the chosen predictors for the final step of the stepwise regression for the binned 12hr forecast equation as an example, illustrating the variability in the predictability as a function of initial intensity and the varying dynamic and thermodynamic factors contributing to that predictability.

d. Summary

Accurately forecasting hurricane intensity remains a challenge even though much progress has been made in improving TC track forecasting. Despite the increasing amount of observations from within the TC core in the Atlantic basin in particular, relatively little research focusing on improved operational intensity forecasting has been performed which utilizes this data. Instead, the majority of TC intensity forecasting studies have focused on the influence of the storm environment and its impacts on intensity change. Advances in computing power have permitted meteorological centers to develop more sophisticated dynamical models (e.g. WRF, HWRF, GFDL); yet, the skill of intensity forecasts from these high-resolution dynamical models still lags that of statistical models. The study performed here has attempted to build on the successes of the SHIPS-style regression model to create a statistical regression scheme (ASPIRE) that utilizes core measurements provided in VDMs to produce TC intensity forecasts from 12 h to 48 h.

A VDM climatology from 1991-2008 was produced which included information such as eye type, eye size, eye diameter, MSLP, temperature, and dewpoint, to name a few parameters. Distributions of each parameter were examined, and their relationship to our understanding of the processes behind rapid intensity change and structural change were explored. An eye structure forecast tool was created through which the expected climatological rate of intensity change can be produced from 12 h to 48 h, given an initial eye diameter from a VDM and an advisory wind speed. These diagrams revealed that TCs with a wind speed of less than (greater than) 95 kt will strengthen (weaken), climatologically. This finding argues that the 95 kt threshold fundamentally represents a transitional intensity in the evolution of a TC. The standard error associated with the mean plots of rate of intensity change was also presented. These plots indicated that there are three intensity regimes with increased variability. The possibility that these regimes may be related to preferred areas for concentric eyewall development and ERCs was discussed. The relationship of the climatological 12-h change in intensity to Sawyer-Eliassen balance was also discussed, offering a potential explanation for the observed tendency of strengthening for TCs with an intensity of less than 95 kt. Simple forecasts using the eye structure tool were created. While these intensity forecasts based solely on climatological

characteristics of TCs gathered from VDMs have limited use in an operational setting, they could prove beneficial as a new verification benchmark for TCs in the Atlantic basin that have an eye. Future work involving these eye structure forecasts will seek to create confidence intervals within which the mean intensity of the TC can be expected to fall with 95% certainty.

A stepwise multiple linear regression scheme to predict TC intensity change in the Atlantic basin (ASPIRE) was also developed. The ASPIRE technique utilized TC inner core measurements reported in VDMs as well as persistence variables. Other thermodynamic predictors and measures of inertial stability were computed and included as potential predictors in an attempt to take full advantage of the available data resources provided in VDMs. Three separate sets of equations were created (TOTAL, NS, and NSNC). Each of these methods had one full equation in which a single equation was used to produce forecasts for TCs of all intensities. Separately, forecast equations using running bins of 20 kt initial intensity were also developed for each of the three methods.

Results of independent testing for the periods from 1997-2002 and 2005-2008 show that the NSNC method of the ASPIRE technique performs reasonably well for independent data. Comparisons of potential predictive ability as measured by the R2pred along with RMSE calculations demonstrated that the binned equations outperform their full regression equation counterparts for virtually every intensity bin at all forecast lead times. Dependent tests of the overall performance of the NSNC models at 12 h shows that storm-scale predictors are likely essential for improving statistical TC intensity forecasting and suggests that the incorporation of TC core measurements into statistical models such as SHIPS could further enhance the quality such forecasts. Regimes of decreased potential predictive ability through the ASPIRE technique—likely associated with concentric eyewalls and ERCs—were evident in Figure 6.12. This figure quickly revealed that the predictability of future TC intensity is strongly a function of the initial intensity of the hurricane, with three minima of forecast confidence evident at the 70 kt, 105 kt, and 140 kt intensities. Figure 6.15 showed that SHIPS exhibits a decrease in skill in these preferred regimes for concentric eyewall formation. At the same time, two areas of increased predictive ability from the SHIPS model located between these concentric regimes were also noted. These results suggest that inner-core data may be required for increased predictability of the onset of concentric eyewall cycles while environmental data is necessary for predicting the amount of strengthening that will occur following an ERC.

The performance of the ASPIRE technique indicates that a new benchmark in statistical TC intensity forecasting may have been attained for forecasts within 24 h, while combination of core predictors utilized in ASPIRE with environmental and oceanic predictors in SHIPS may improve

forecasts from 24 h to 48 h. However, without extensive testing of ASPIRE on independent data, no definitive conclusions on the effectiveness of this model can be drawn as of yet. The rather inactive 2009 Atlantic hurricane season precluded independent real-time testing of the ASPIRE technique from being performed. However, preliminary independent results from Hurricane Bill (not shown) indicate that the NSNC method of the ASPIRE technique was superior to SHIPS model guidance and comparable to NHC OFCL forecasts. Future work with the ASPIRE technique will seek to expand the version detailed in this study to create a new regression scheme valid for tropical systems of weaker intensities. Rather than using 700 hPa flight level data, that work will focus on 850 hPa flight level data and will attempt to utilize core measurements of temperature and dewpoint in a new regression scheme to predict TC intensity change. A regression developed specifically for concentric and elliptical eyewalls may improve the accuracy of TC intensity forecasts for TCs undergoing ERCs. The ASPIRE technique may also see additional improvement beyond that described in this study through the inclusion of predictors such as vertical wind shear, upper-level divergence, and OHC. Finally, the ASPIRE technique may be able to be expanded to other ocean basins where recon flights are not currently flown, such as the West Pacific, through the use of satellite data to create proxy VDMs.

e. References

DeMaria, M., and J. Kaplan, 1994: A Statistical Hurricane Intensity Prediction Scheme (SHIPS) for the Atlantic Basin. Wea. Forecasting, 9, 209–220.

----------, and J. Kaplan, 1999: An Updated Statistical Hurricane Intensity Prediction Scheme (SHIPS) for the Atlantic and Eastern North Pacific Basins. Wea. Forecasting, 14, 326–337.

Eliassen, A., 1951: Slow Thermally or Frictionally Controlled Meridional Circulation in a Circular Vortex. Astrophys. Norv., 5, 19-60.

Piech, D., 2007: Atlantic Reconnaissance Vortex Message Climatology and Composites and Their Use in Characterizing Eyewall Cycles. M.S. Thesis, Florida State University, 139 pp.

Rappaport, E.N., et al., 2009: Advances and Challenges at the National Hurricane Center. Wea. Forecasting, 24, 395–419.

Shapiro, L.J., and H.E. Willoughby, 1982: The Response of Balanced Hurricanes to Local Sources of Heat and Momentum. J. Atmos. Sci., 39, 378–394.

Wilks, D.S., 2006: Statistical Methods in the Atmospheric Sciences. 2nd ed. International Geophysics Series, Vol. 91, Academic Press, 627 pp.

Willoughby, H., J. Clos, and M. Shoreibah, 1982: Concentric Eye Walls, Secondary Wind Maxima, and The Evolution of the Hurricane vortex. J. Atmos. Sci., 39, 395–411.

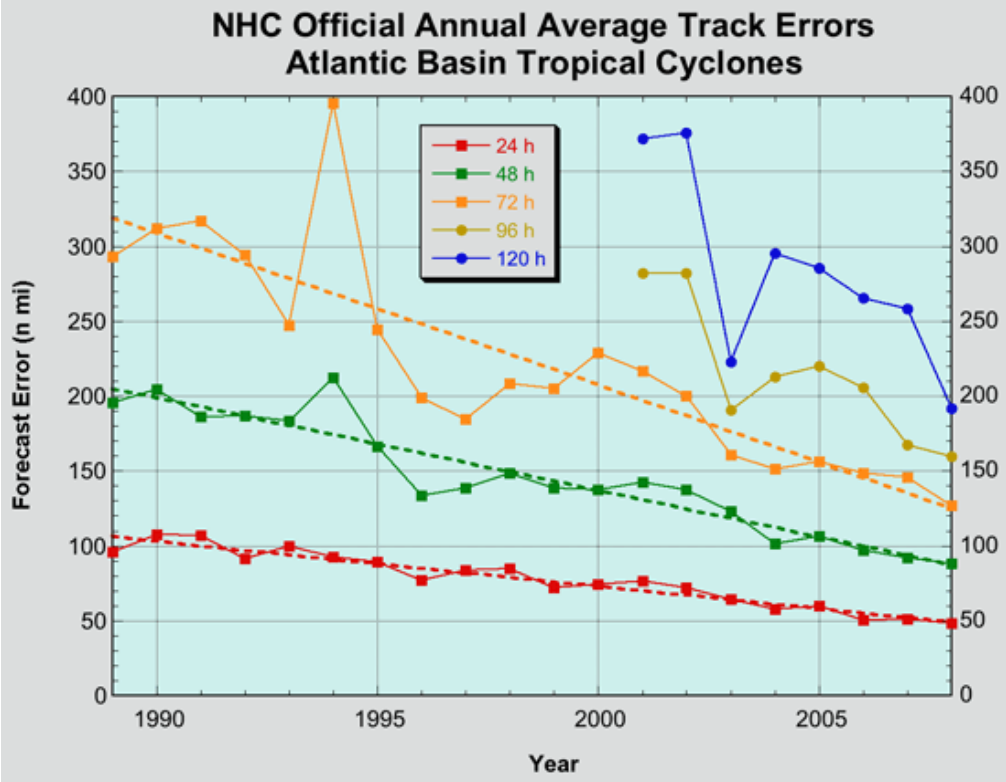

Figure 1.1: NHC official forecast annual average track errors for 1989-2008 with least-squares trendlines superimposed, courtesy of NHC (http://www.nhc.noaa.gov/verification/verify5.shtml).

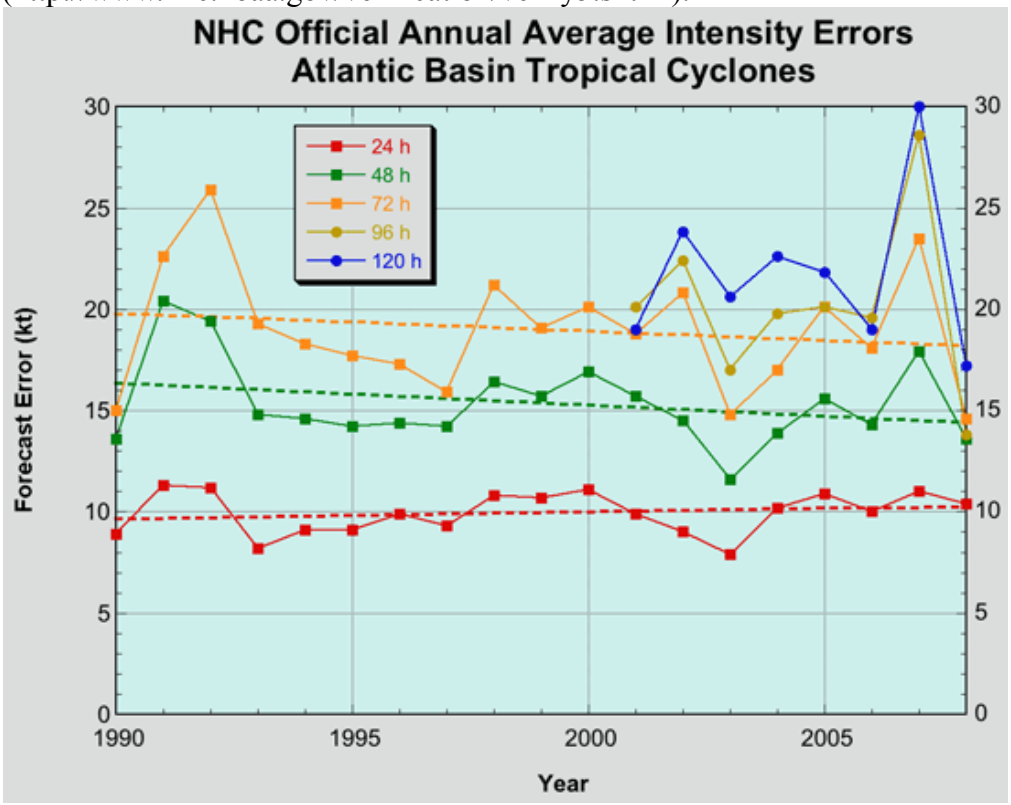

Figure 1.2: NHC official forecast annual average intensity errors for 1990-2008 with least-squares trendlines superimposed, courtesy of NHC (http://www.nhc.noaa.gov/verification/verify5.shtml).

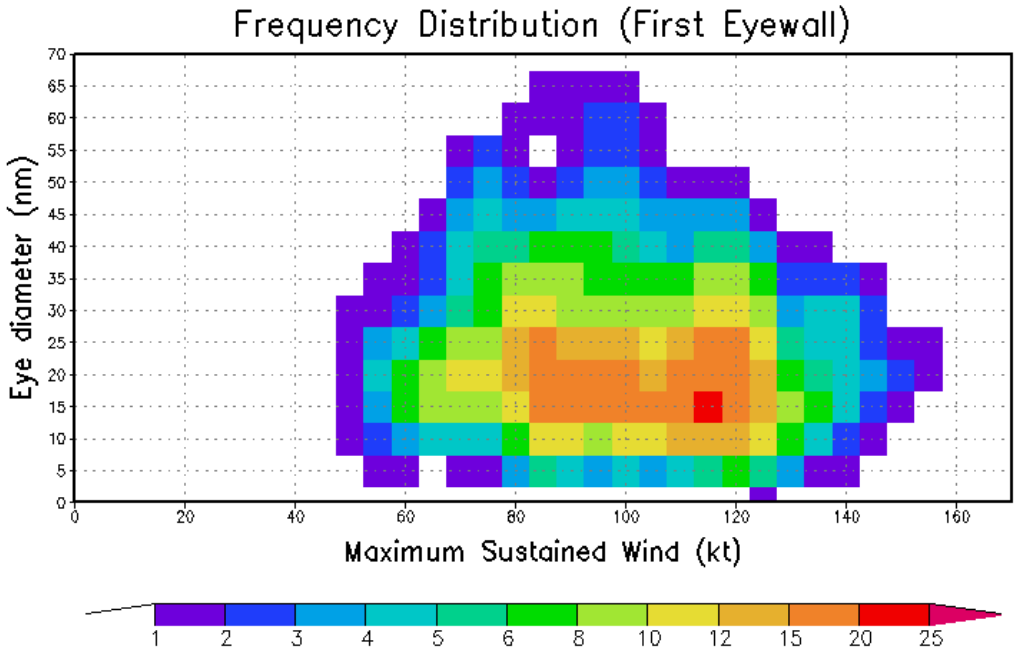

Figure 1.3: 1989-2008 climatology of hurricane eye existence as a function of NHC advisory wind speed (kt) and reconnaissance vortex message eye diameter (nm).

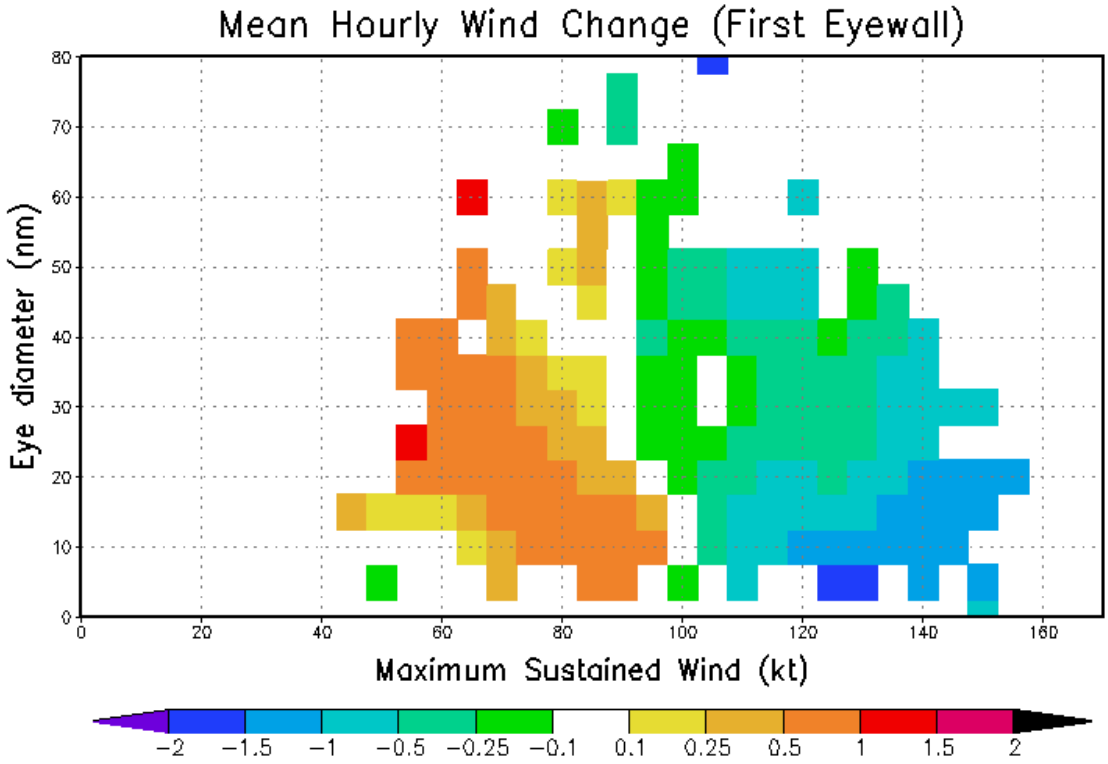

Figure 1.4: 1989-2008 climatological mean hourly intensity change (kt) following a reconnaissance observation for a given initial wind speed and eye size.

Predictor Abbreviation	Predictor Description
1stAdvAge	Seconds since first advisory issued
1stTSAge	Seconds since becoming tropical storm status
Area*dTd	Area of eye multiplied by the prior change in the eye dewpoint
Area*dTi	Area of eye multiplied by the prior change in the eye temperature
Cos(lat)*wind	Cosine of latitude multiplied by advisory wind speed
Cos(Lat)/MSLP	Cosine of latitude divided by recon MSLP
Dewpointchange	Prior change in the dewpoint in the eye
Diam1change	Prior change in the diameter of the eye
Diff_theta	Prior change in eye potential temperature
Difftemp	Prior change in eye temperature
Eyetempi	Temperature of eye at flight level
Eyetempichange	Prior temperature change of eye temperature
Eyetempo	Temperature of air just outside eyewall
Eyetempochange	Prior temperature change of air just outside eyewall at flight level
Jday	Julian Day
Lat	Latitude
Lat*Lon	Latitude multiplied by Longitude
Lon	Longitude
MSLP	Mean sea level pressure by recon
New_Eyetype	Type of eye: 1=Elliptical, 2=Circular, 3=Concentric
Prev12wind	12hour Prior advisory wind change
Prev6diff	Prior 6Hour change in advisory wind
Prev6wind	6Hour Prior advisory wind change
Prevp12diff	12Hour prior change in recon MSLP
Prevp6diff	6Hour prior change in recon MSLP
S-Fcst	Difference between climatology forecast (Fcst) and ships forecast (S)
SHIPS	SHIPS forecast issued at or prior to advisory
Sin(Lat)*Wind	Sine of latitude multiplied by advisory wind
Sin(Lat)/MSLP	Sine of latitude divided by MSLP
Theta	Potential temperature of the eye at flight level
Thetae	Equivalent potential temperature of the eye at flight level
Thetae-Theta	Difference between eye equivalent potential temperature and pot. temperature
Time_day	Local hour of the day
V^2/R	Advisory wind speed squared divided by eye radius
Wind	Advisory wind at or prior to the recon time
Wind*Prev12Diff	Advisory wind multiplied by the prior 12hour change in advisory wind
Wind*prev6diff	Advisory wind multiplied by prior 6hour change in advisory wind

Figure 1.5: Table of predictors chosen for stepwise regression in at least one forecast time. Before regression is performed, all predictors are transformed to become approximately normally distributed using either logarithms or exponentials of various bases (see Figure 1.4 for example). Approximately two dozen additional predictors were tested but never chosen in the final regression equation, and thus are not listed above.

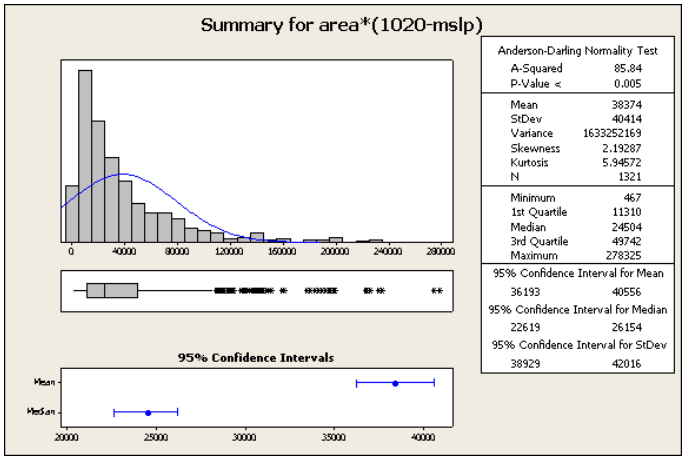

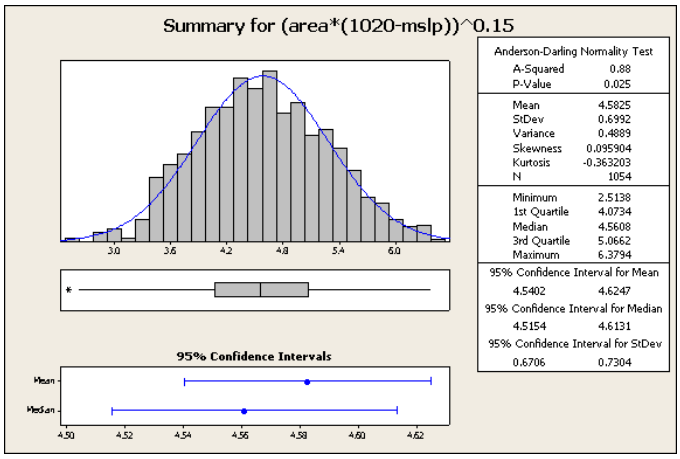

Figure 1.6: Example of transformation of highly non-Gaussian predictor (left; area of eye multiplied by 1020-mean sea level pressure)) to an approximately normal distribution (right; the same variable raised to the power 0.15).

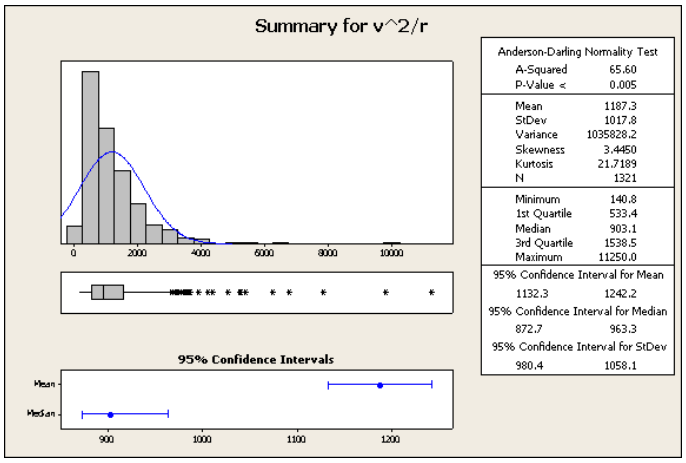

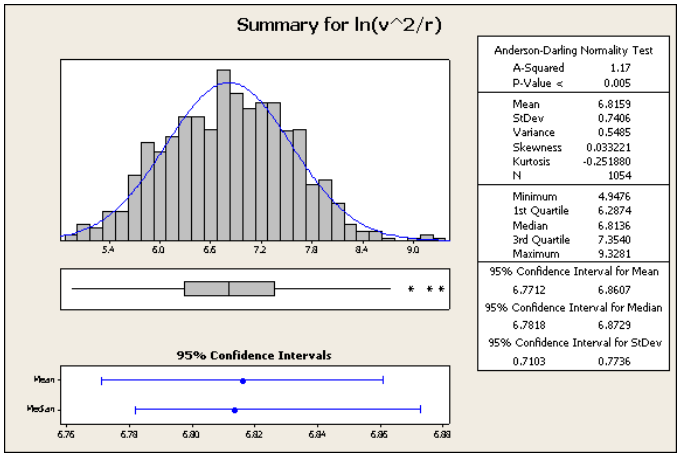

Figure 1.7: Example of transformation of highly non-Gaussian predictor (left; V^2/r, the centrifugal acceleration) to an approximately normal distribution (right; the natural logarithm of the same variable).

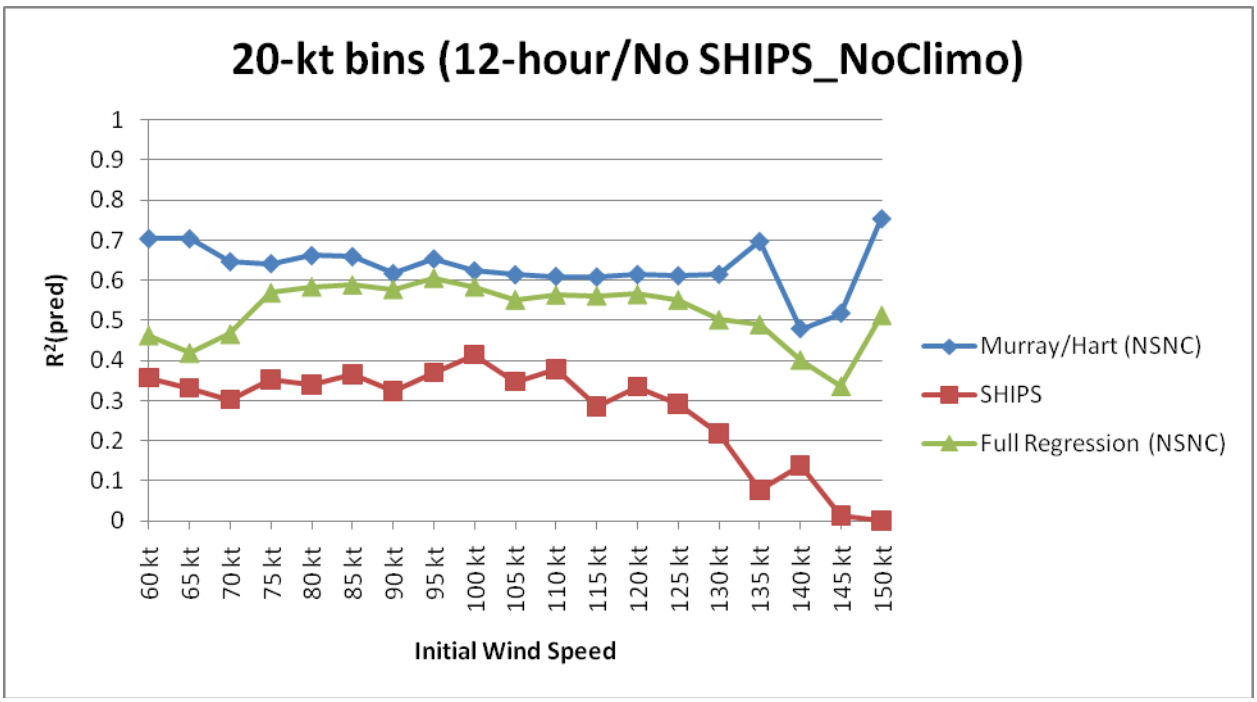

Figure 1.8: Out-of-sample (cross validation) R-squared for 12-hour forecast of hurricane intensity (wind speed) for red: SHIPS forecast, green: full regression using entire database, and blue: regression using a 20-kt bin database. The blue forecast here does not utilize SHIPS or the climatology in Fig. 1.2 in its forecast. Note the extremely significant improvement over SHIPS by both the green and blue lines in this figure and those that follow.

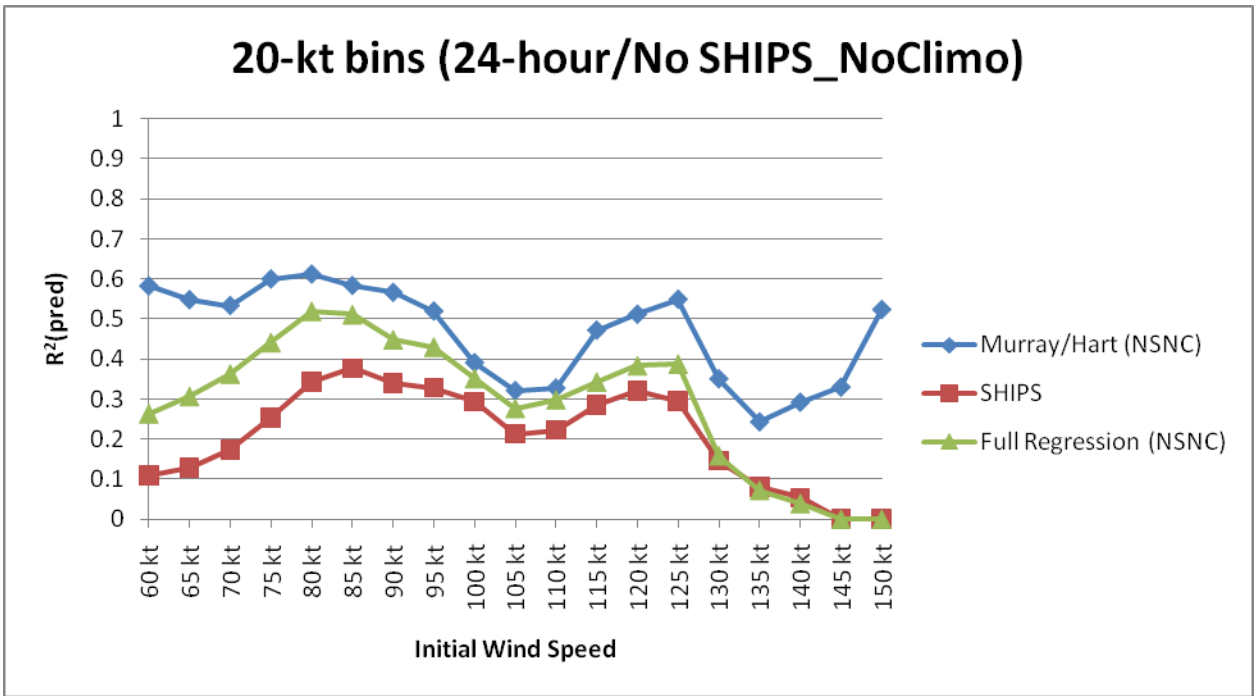

Figure 1.9: As in Figure 1.4, except for a 24-hour forecast.

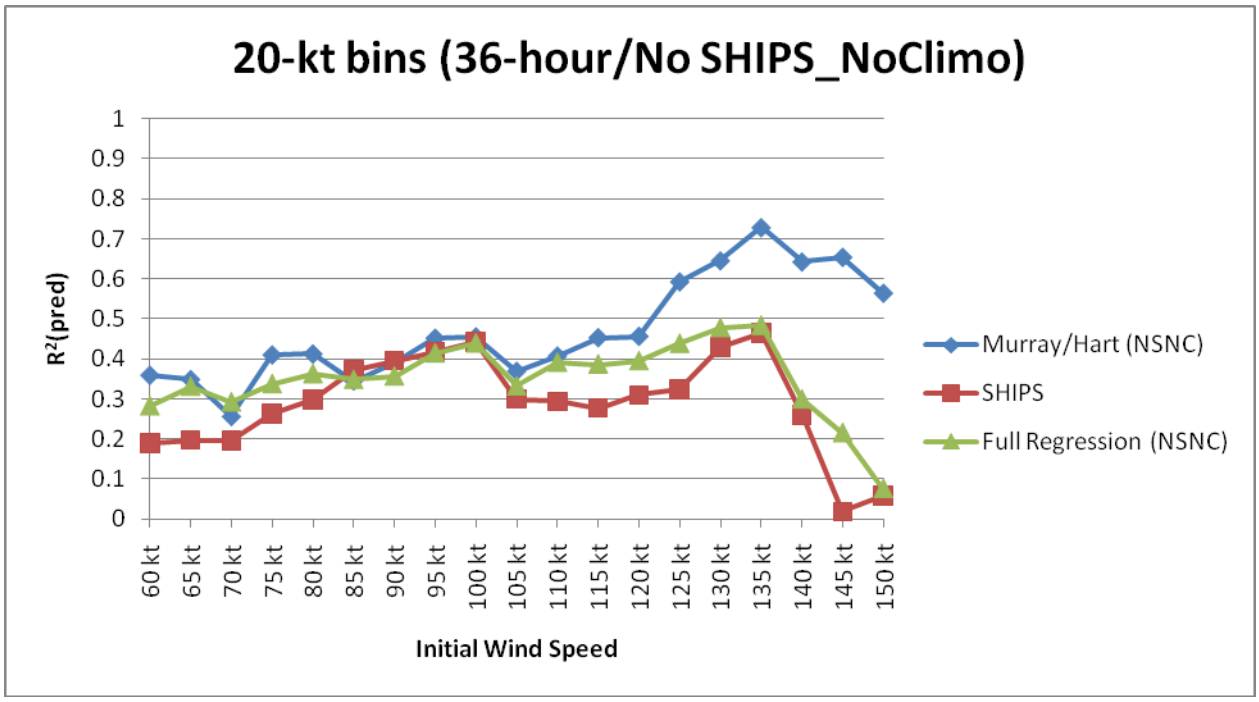

Figure 1.10: As in Figure 1.4, except for a 36-hour forecast.

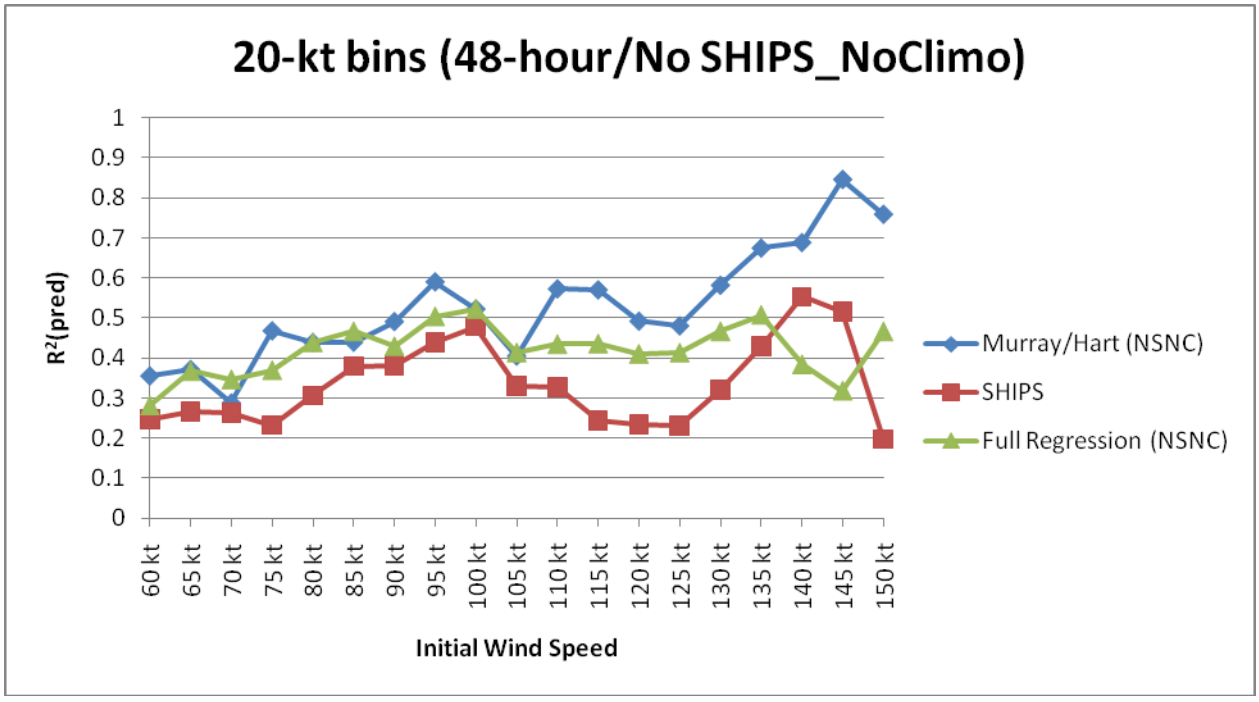

Figure 1.11: As in Figure 1.4, except for a 48-hour forecast.

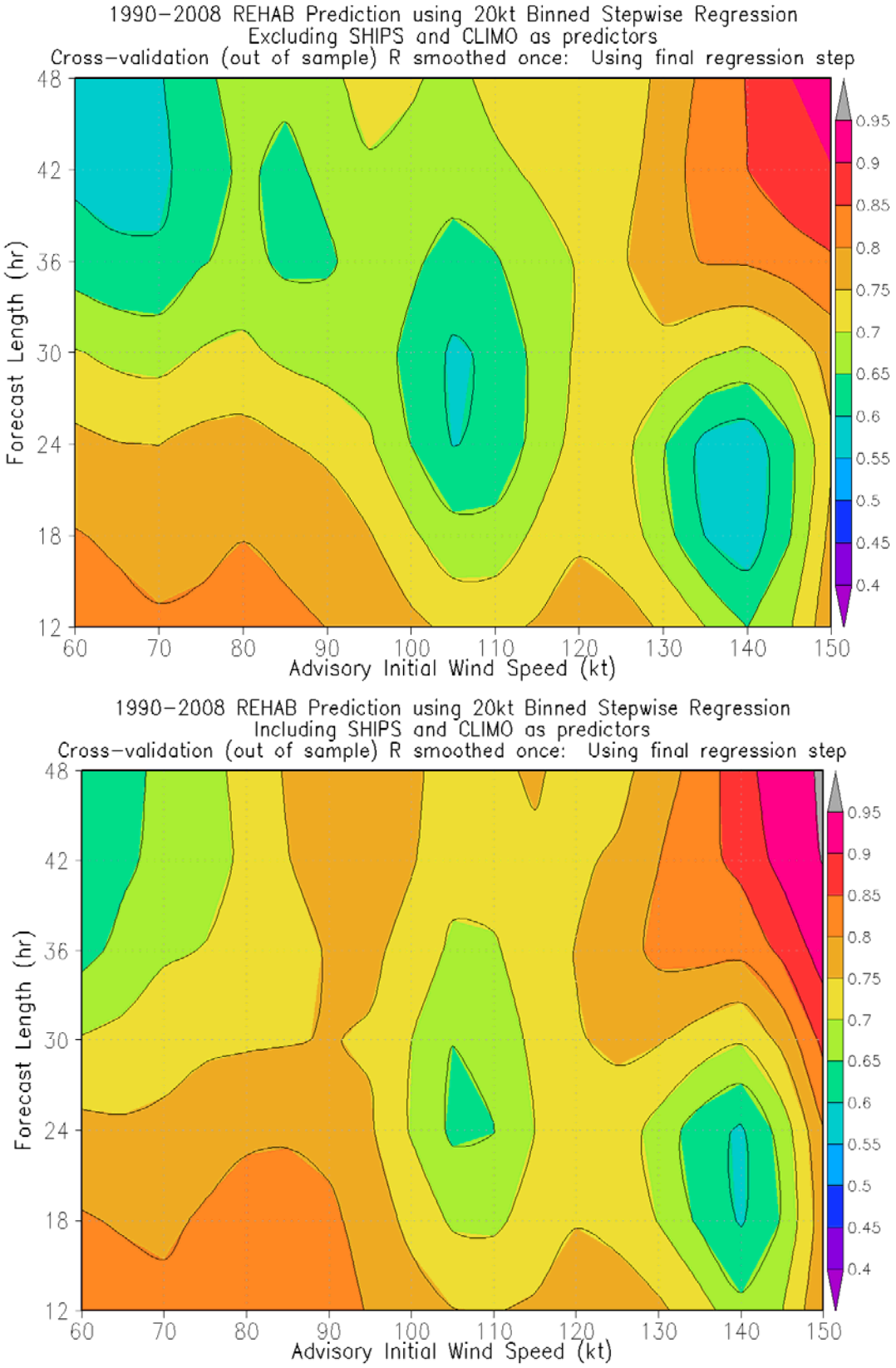

Figure 1.12: A shaded plot that synthesizes the out-of-sample (cross-validation) forecast performance (Rsquared-predicted) as a function of initial wind speed and forecast length for the 20kt binned stepwise regression. Top) Excluding SHIPS and CLIMO as predictors and Bottom) Including SHIPS and CLIMO as predictors. A nine-point smoother was applied to both images.

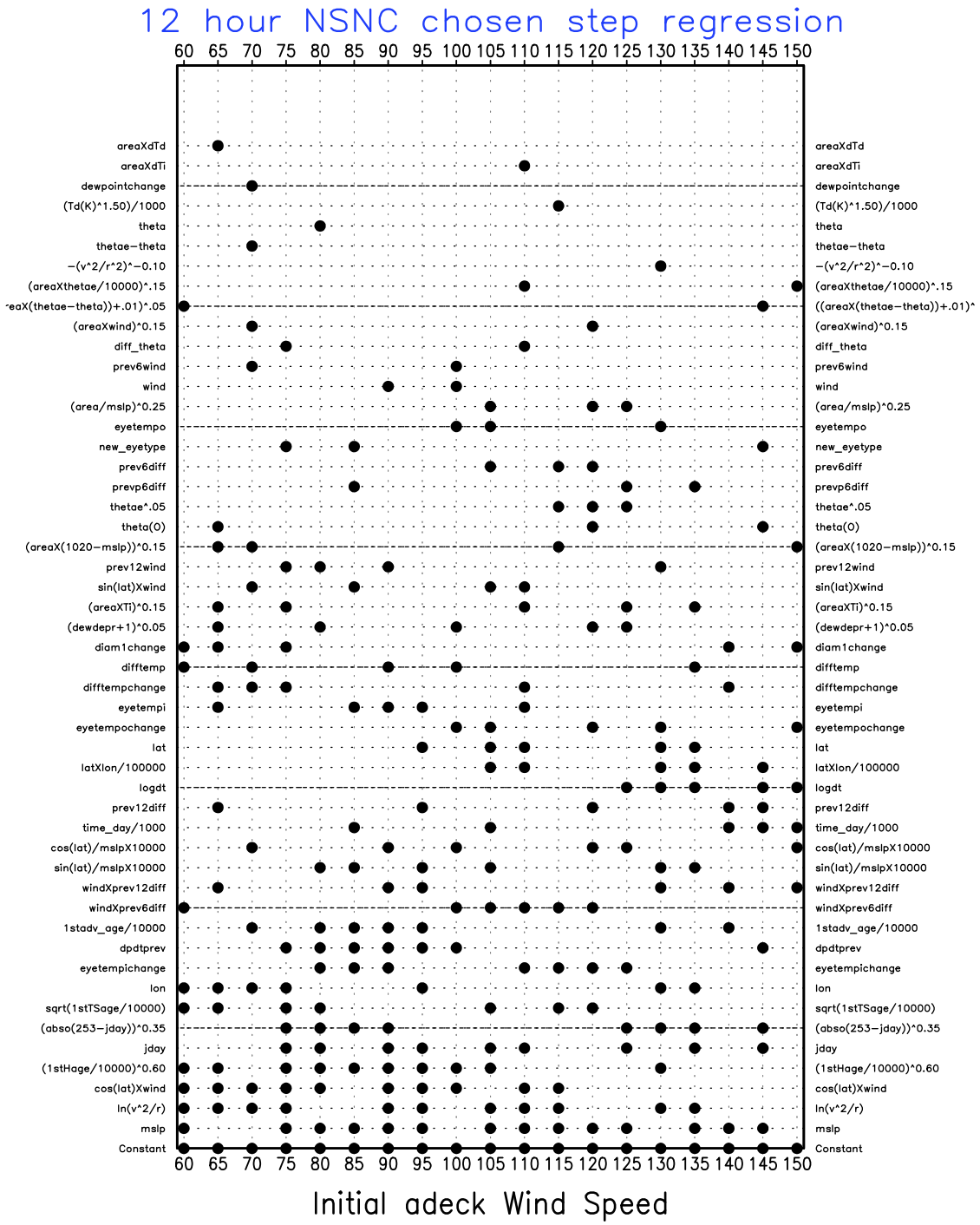

Figure 1.13: Predictors chosen in at the final step of stepwise regression at 12hr forecast as a function of initial wind speed. Please see text and Murray (2009) thesis for a description of the predictors on the axes.

FINAL REPORT OF THE SUBPROJECT ENTITLED:

"Developing a parameter for forecasting tornadoes in landfalling tropical cyclones."

By

HENRY E. FUELBERG, PI
MATTHEW ONDERLINDE, GRADUATE STUDENT

1. Background and Objectives

Approximately 47 tropical systems have affected the Gulf of Mexico region since 2000, including 26 that impacted the state of Florida. While the effects of tropical cyclone (TC) winds near the storm center are widely known, the most damaging effects at locations farther from the center often result from severe local storms (Schultz and Cecil 2009). These include tornadoes or high wind events such as downbursts that can produce substantial damage hundreds of kilometers from the cyclone's center of circulation. For example, the rainband in Hurricane Ivan (2004) that was responsible for widespread tornadoes during landfall was located between approximately 250 and 450 km from the storm's center (Baker et al. 2009). The threat for severe storms may last as long as three days after cyclone landfall, and as far as 500 km from the cyclone's center. Thus, severe local storms put locations at risk that might otherwise avoid damage from the TC. Although TC-related tornadoes comprised only about 3.4% of the total number of reported tornadoes since 1950, they contributed approximately $1.4 billion to the tornado damage total (~ 5% of all U.S. tornado monetary damage).

The conditions in which tornadoes develop near tropical cyclones are somewhat different from the very unstable and highly sheared tornado environments of the Great Plains (e.g., McCaul 1991; Edwards 2008). Although atmospheric conditions such as wind shear and instability probably are crucial to tornado development in either environment, subtle differences do exist. For example, TCs typically exhibit highly sheared environments but with only modest instability (Novlan and Gray 1974; McCaul 1991; Bogner et al. 2000; Baker et al. 2009). Even though measures of instability such as Convective Available Potential Energy (CAPE) typically are small, supercells (rotating thunderstorms) appear to be the most common mechanism for tornadogenesis (e.g., McCaul 1987; Spratt et al. 1997; Suzuki et al. 2000; McCaul et al. 2004; Edwards 2008). These TC-related supercells often are shallower and smaller than their mid-latitude counterparts (McCaul and Weisman 1996).

Related to the forecasting problem is the public's perception of risk during a tropical cyclone event. Forecasters often are faced with the problem of forecasting what they believe will occur versus what will generate the appropriate response from the public. While the effects of storm surge and high winds may be well accepted and understood by the public, the risk of severe local storms at large radii may be less recognized. Therefore, it is critical to provide accurate forecasts of all hazards related to TCs, both direct (surge, storm core high winds, etc.) and indirect (severe local storms at large radii).

The objective of this study has been to develop a statistical guidance product to forecast the frequency of tornadoes during a landfalling tropical cyclone. We have collaborated closely with personnel at the National Weather Service's (NWS) Storm Prediction Center (SPC) . We hypothesized

that a composite parameter similar to those derived for forecasting tornadoes in classical severe storms could be developed for the tropical cyclone environment and that it would produce more accurate forecasts of tornado occurrence. This hypothesis assumed that the classic parameters do not adequately consider the conditions that lead to tornado formation in TCs.

2. Methodology

We used two quality controlled data sets from the NWS as well as Rapid Update Cycle (RUC) model data (Benjamin et al. 2002; Benjamin et al. 1994) from the National Centers for Environmental Predictions (NCEP). The first NWS dataset was the National Hurricane Center's (NHC) best track data (Jarvinen et al. 1984). We used data from 2000 through 2008 because of RUC model changes that occurred prior to that period. The second data source was SPC's ONETOR tornado reports. The SPC compiles storm reports for the United States on a daily basis; however, the initial reports are highly prone to error and multiple reporting (multiple reports of the same tornado). To alleviate this issue, the SPC and National Climate Data Center (NCDC) perform a careful post-analysis to obtain the most accurate final dataset. ONETOR contains extensive information about each tornado.

The NHC best track data were combined with the SPC ONETOR data to consolidate all of the variables relevant to TC tornadogenesis. First, a subsetted region was selected to restrict the analysis to TC-related tornadoes that were relatively close to the time of TC landfall. This region encompassed the area between 24.1 - 35.6^{o}N and 79.1 - 101.4°W, incorporating all of the northern Gulf of Mexico and east coast of Florida. The second step was to locate all tornadoes between 200 and 750 km of TCs in the subset region and within 3 h of a best track TC time. Because of the difficulty in discerning between TC wind damage and tornado damage in the TC's core region, we did not consider tornado reports within 200 km of the eye. The 750 km value helped alleviate the problem of determining whether a tornado report outside of this range was due solely to the TC.

We used multiple linear regression (Wilks 2006) to forecast the formation of TC tornadoes. As a first step, we defined the dependent variable to be the number of tornadoes occurring in each quadrant of a TC during a 12 h interval. This time interval includes tornadoes occurring 6 h before to 6 h after the forecast time. Thus, we assumed that tornadoes in this entire interval are related to conditions at the forecast time (the center of the 12 h interval). Each reported tornado that met these criteria and was located between 200 – 750 km of the TC's center was tallied. A total of 483 tornado reports associated with 30 TCs met the criteria. Units of the dependent variable are the number of tornadoes between 200 - 750 km of the TC in the given quadrant per 12 h period.

Each independent variable was evaluated based on its physical and statistical relevance to the tornado reports. The first group described the location and timing of the TC and tornado report. Examples are hours from landfall and distance from the TC to the tornado report. The remaining variables were atmospheric parameters derived from the RUC analyses that are known to be related to tornado formation.

We also defined 240 null cases in which no tornadoes occurred. A null case was a location where no tornadoes occurred within a 12 h interval, and no tornadoes occurred in the entire TC quadrant containing the null location during this 12 h interval. The null cases were evenly distributed between the 30 storms so each storm contributed 8 cases. Null cases were randomly located around the TC, taking care not to select locations in quadrants where tornadoes were reported during the same 12 h interval.

We used stepwise multiple linear regression (Wilks 2006) to analyze and select the variables related to tornadoes in the TC environment. However before using regression, inter-correlations between the potential independent variables were examined to insure that the final equation would not be over-fit to the data. Each potential variable also was scrutinized to determine if it had physical relevance and a correlation sign (positive vs. negative) that was appropriate. Once these steps were completed, thirty passes were made through the data, with stepwise regression used to generate an equation from the 29 storms of each pass. Thus, each storm was omitted once in the total procedure. The variables that were accepted or rejected based on their significance (p-value ≤ 0.05) could vary from run to run so that different passes could yield different sets of variables. After completing the cross validation procedure, the final variables were selected based on the frequency that they were significant during the 30 passes. With only two exceptions, the variables selected by cross validation were the same, and only small variations were noted between the coefficients of the different passes. Therefore, seven "final" variables were retained. Then, the coefficients from the 28 passes in which the significant variables were the same were averaged to yield the final coefficients for the equation defining our Tropical Cyclone Tornado Parameter (TCTP).

3. Results

Table 1 shows the seven final predictors that comprise the TCTP equation, along with their correlations with the number of tornadoes, coefficients in the equation, means, and standard deviations. The predictors are ordered from largest to smallest correlation with the tornado reports to indicate the relative importance of each term. The means and standard deviations were calculated without

including the null cases; therefore, the statistics represent only the TC-related tornado events.

Table 1. The seven final predictors and their correlation with tornado reports, their regression coefficient, mean, and standard deviation.

PREDICTOR	Correlation with tornadoes	Regression Coefficient	Mean	Standard Deviation
0-3 km shear (kt)	0.508	0.1439	30	8.3
0-3 km storm relative helicity ($m^2 s^{-2}$)	0.501	0.0198	127	83.5
Sine azimuth angle	0.478	4.3721	0.83	0.28
Hour of the day	0.270	0.3193	12.1	5.1
RUC-defined CAPE ($J kg^{-1}$)	-0.209	-0.0014	782	567
TC max sustained winds (kt)	0.169	0.0312	54.3	29.8
Hours after (before) landfall	0.159	0.0218	5.0	17.5
Constant	—	-3.5587	—	—

Five individual TCs were analyzed in detail. Hurricanes Ike (2008) and Charley (2004) were selected for their relative sizes. Ike was a large TC, while Charley was fairly small. It also was desirable to cover a wide range of TC intensities in the five cases. Charley was a category 4 storm at landfall, Ike a category 2, Cindy (2005) a minimal category 1, and Barry (2007) peaked in the tropical storm range. Barry also was considered because of its lack of tornado production. While some tropical storms in the final data set contributed 15 or more tornadoes, Barry contributed only two. Finally, Hurricane Frances (2004) was considered since it produced the most tornadoes (78) in the study. For the sake of brevity, only results for Hurricanes Charley (2004) and Frances (2004) are presented here.

Statistics for tornado reports in the northeast quadrants of TCs were calculated (Table 2) to compare conditions when tornadoes did or did not occur (the null cases). Most values for the tornado cases are considerably different from those of the null cases.

Table 1. Mean values for tornado reports vs. the null cases in the northeast quadrant. There were 287 tornado reports and 99 null cases in the northeast quadrants.

Parameter	Mean of Tornado Cases		Mean of Null Cases

0-3 km Shear (kt)	31.3		16.4
0-3 km SRH ($m^2 s^{-2}$)	135		50
RUC CAPE ($J kg^{-1}$)	650		1090
TC max sustained wind (kt)	65		52
Hours after landfall	4.5		-8.2

A. Case 1 – Hurricane Charley (2004)

Hurricane Charley began as a depression in the southeastern Caribbean on 9 August 2004. After passing over western Cuba and approaching the Florida peninsula as a category 2 storm, Charley intensified to category 4 status just before making landfall south of Tampa, FL at approximately 2000 UTC 13 August. The storm then quickly crossed the Florida peninsula and briefly re-emerged over the Atlantic before making a second landfall south of the border between North and South Carolina. Charley was a compact, intense storm at landfall with maximum sustained winds of 125 kt. It maintained hurricane strength as it crossed Florida and was a minimum category 1 hurricane with winds of 65 kt at second landfall. Charley contributed 17 tornadoes to the study, including 3 EF-2 tornadoes.

Figure 1 is a time series of TCTP from 0000 UTC 13 August to 0600 UTC 14 August. The greatest TCTP forecasts, from 1200 to 1800 UTC 13 August, correspond well with maximum tornado production during these hours (12.1 tornadoes forecast with 14 reported from 0600 to 1800 UTC, and 14.3 tornadoes forecast with 10 reported from 1200 to 0000 UTC). However, large areas of 2-6 tornado forecasts are located where few or no tornadoes actually occur. We believe that the large contribution from the term "sine of tornado azimuth" (coefficient of 4.372, Table 1) produces these regions, particularly in the northeast and southeast quadrants where the term is largest. TCTP values peak over land areas due to large low-level shear in the boundary layer.

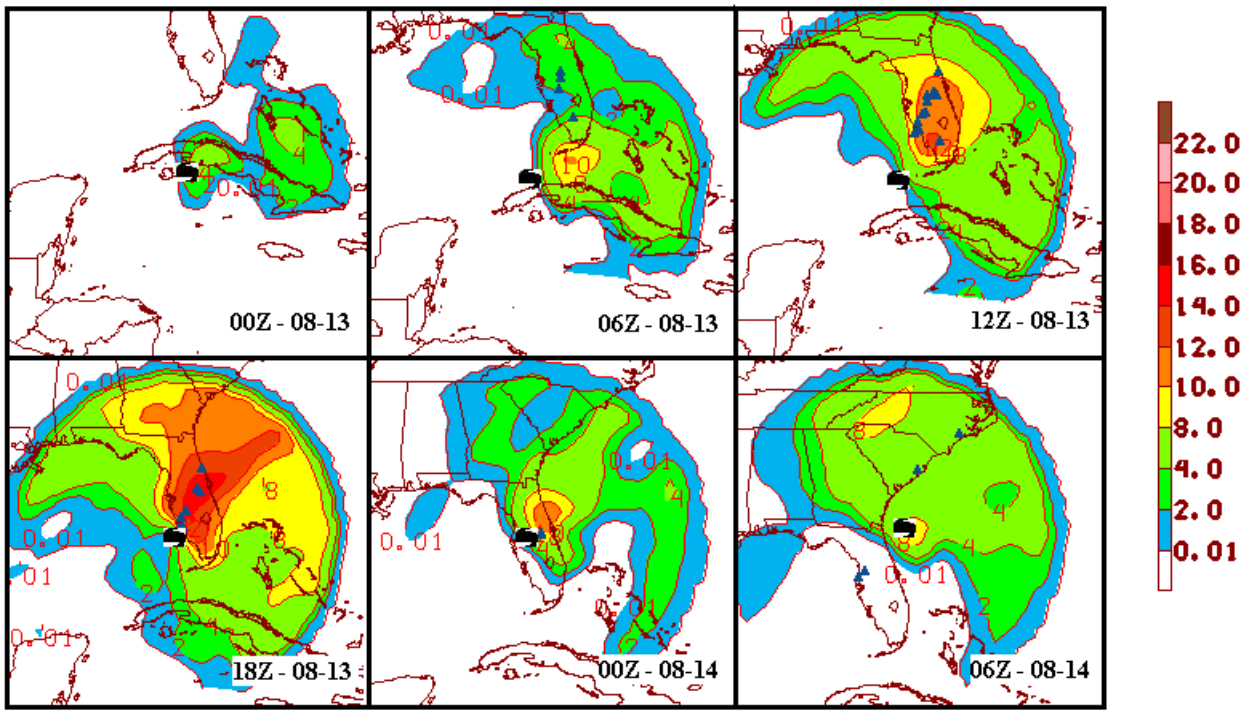

Figure 2. *Time series of TCTP from 0000 UTC 13 August 2004 (upper-right) to 0600 UTC 14 August (lower right) during Charley. Blue triangles represent locations of tornado reports from 6 h before to 6 h after each forecast time. The units of TCTP are the number of tornadoes in a quadrant (200-750 km radius) per 12 h. Charley's locations are indicated.*

TCTP forecasts well when compared to traditional tornado guidance products. Figure 2 compares patterns of the Energy Helicity Index (EHI), Significant Tornado Parameter (STP), and TCTP. Compared to STP and EHI, maxima in TCTP correspond best with tornado occurrence during Charley. Conversely, the STP and EHI parameters highlight areas over South Florida at both 1200 and 1800 UTC 13 August where tornadoes do not occur. However, we note that STP and EHI were designed to forecast only strong tornadoes.

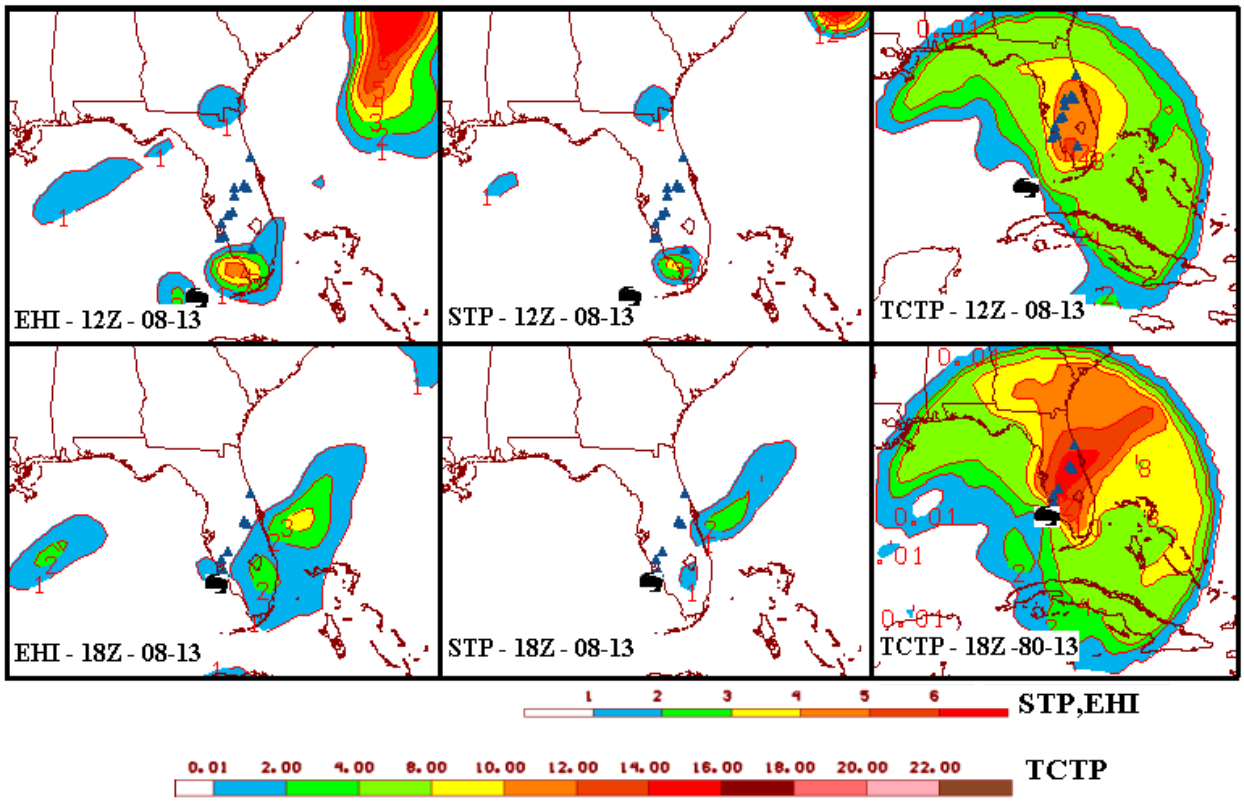

Figure 3*. Energy-Helicity Index (EHI), Significant Tornado Parameter (STP), and Tropical Cyclone Tornado Parameter (TCTP) for Hurricane Charley at 1200 and 1800 UTC 13 August 2004. Blue triangles represent locations of tornado reports from 6 h before to 6 h after both forecast times. The units of TCTP are the number of tornadoes in a quadrant (200-750 km radius) per 12 h. Charley's locations are indicated.*

B. Case 2 – Hurricane Frances (2004)

Hurricane Frances is examined since it produced the most tornadoes (78 tornadoes, 5 EF-2, 1 EF-3) of any storm comprising the study. Frances developed from a tropical wave that moved off the coast of Africa. After traveling west-northwestward across the Atlantic, Frances made its first landfall at the southern end of Hutchinson Island, FL at 1800 UTC 6 September as a category 2 hurricane with maximum winds of 90 kt. After briefly emerging over the far northeastern Gulf, the storm proceeded north-northeastward along the Appalachian Mountains, finally dissipating over the Gulf of St. Lawrence on 10 September.

Although Frances produced 15 tornadoes on its day of landfall (6 September), tornado activity peaked on 7 September when 52 of its 78 tornadoes occurred. CAPE remained modest during Frances, as in previous cases, with only 13 of the 52 tornadoes on 7 September exhibiting values greater than 1000 J kg^{-1}. Wind shear between the surface and 3 km frequently peaked above 40 kt in Frances'

northeast quadrant on 7 September; however, only 18 of 52 tornadoes were associated with values greater than 30 kt. Similarly, the shear often peaked above 300 m^2 s^{-2}, although only 9 tornadoes were associated with SRH03 greater than 200 m^2 s^{-2}.

Figure 4 shows a time series of TCTP from 1800 UTC 6 September to 0000 UTC 8 September. TCTP under-forecasts tornadoes during Frances' peak production period of 0600 to 1800 UTC 7 September. However, it slightly over-forecasts outside of this time period (e.g., 16.2 forecast when 4 are observed at 1800 UTC 6 September). Values less than 16 are forecast at 0600, 1200, and 1800 UTC when 33, 34, and 21 tornadoes, respectively, are reported (from 6 h before to 6 h after each forecast time). It again is difficult to explain the over-forecasts during Frances. The mean RUC-derived shear for Frances' tornadoes was 130 m^2 s^{-2}. Mean CAPE during Frances' tornadoes was 890 J kg^{-1}. Although TCTP under-forecasts Frances' peak production period, forecast values are larger compared to previous cases when fewer tornadoes occurred. We believe that TCTP's under-forecasts are due to the statistical scheme used to derive the TCTP equation. Because the equation was derived to forecast all ranges of TC-related tornado productivity, it tends to over-forecast anomalously unproductive TCs and under-forecast anomalously productive ones.

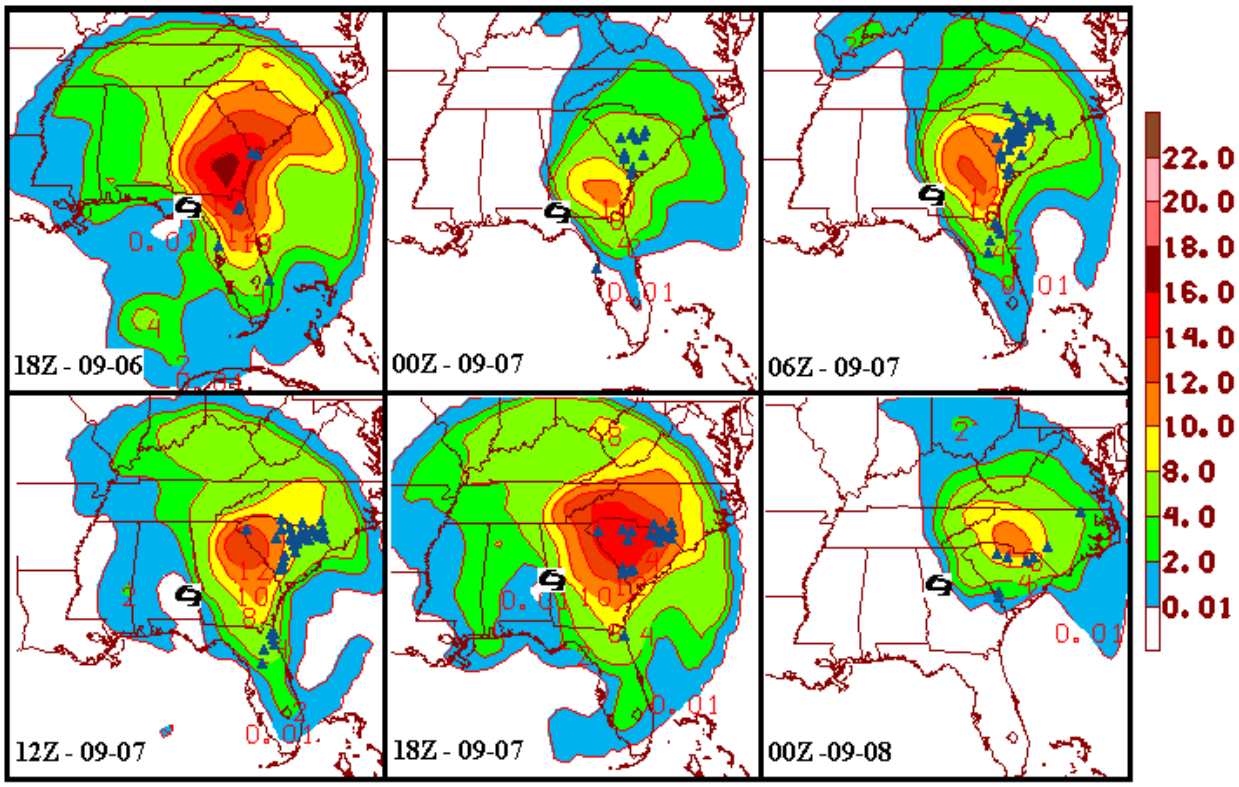

Figure 4. *Time series of TCTP from 1800 UTC 6 September 2004 (upper-right) to 0000 UTC 8*

September (lower right) during Frances. Blue triangles represent locations of tornado reports from 6 h before to 6 h after each forecast time. The units of TCTP are the number of tornadoes in a quadrant (200-750 km radius) per 12 h. Frances' locations are indicated.

4. Summary

This study has developed a composite statistical parameter to use as guidance for forecasting the occurrence of tornadoes in tropical cyclone (TC) environments. We hypothesized that a composite index tuned specifically to the TC environment would outperform indices developed for classical severe storms. A total of 483 TC related tornado reports from 30 storms occurring between the years 2000 to 2008 was used along with 240 null reports from the same storms. These cases comprised our dependent variable. Geographic parameters described the locations and timing of the tornadoes with respect to the parent TC. In addition, a pool of potential TC environment parameters was obtained from RUC model analyses. They included measures of temperature, humidity, stability, and wind shear. Stepwise multiple linear regression then was used to isolate the seven parameters that were best related to tornado occurrence from an original pool of 28. The resulting equation comprised our final Tropical Cyclone Tornado Parameter (TCTP).

TCTP was applied to five tropical systems that varied in size, intensity, and the number of tornadoes that they produced. These storms included Hurricanes Ike (2008), Charley (2004), Cindy (2005), and Frances (2004), as well as Tropical Storm Barry (2007). Forecast tornado occurrence was compared with the number of tornadoes that actually occurred and with those from the Significant Tornado Parameter (STP) and the Energy Helicity Index (EHI) that were designed by the Storm Prediction Center for use in non-tropical environments.

Results of the five TC cases suggest several general findings.

- TCTP appears biased to over-forecast the number of tornadoes that occur, especially when values of shear exceed 250 $m^2 s^{-2}$.
- The shear terms in TCTP were most correlated with tornado occurrence. Instability was weakly negatively correlated with tornado occurrence, as in McCaul (1991).
- Values of shear and helicity were much greater for tornado events than for null cases in the northeast quadrant of our TCs. Conversely, values of TC-related variables such as storm intensity and time from landfall were similar for both tornado and null cases.
- Values of RUC-derived shear and helicity were greatest over land areas during TC landfall, leading to somewhat greater TCTP forecasts. This seems intuitive since boundary layer friction over land is much greater than over water, leading to greater low-level shear.

- Subjective analyses of TCTP forecasts suggest that they adequately identified regions where tornado potential was greatest, but their ability to quantify the number of tornadoes that would occur in a given quadrant was not as good.
- TCTP generally exhibited good continuity between 6 h periods, increasing during times when tornado occurrence increases and decreasing otherwise.
- TCTP consistently recognized the northeast quadrant of TCs as the region of maximum tornado potential, agreeing with previous climatologies (Sadowski 1962; Smith 1965; Pearson and Sadowski 1965; Hill et al. 1966; Novlan and Gray 1974; Gentry 1983; McCaul 1991; Verbout et al. 2007; Schultz and Cecil 2009). However, TCTP also consistently forecast large areas of much smaller number of tornadoes (2-6) in other quadrants where they are not expected and did not occur. This was especially common at azimuths of 120 to 210°.
- TCTP performs well compared to STP and EHI in tropical environments. These initial results suggest that TCTP produced the best tornado forecasts for TCs that made landfall as hurricanes. However, these SPC-derived parameters forecast the likelihood of "significant" tornadoes (EF2 or greater), whereas we included all tornadoes in deriving TCTP. Since most TC-related tornadoes are weaker than EF-2 intensity, it could be argued that the STP forecasts verify accurately in the five cases that we examined since Cindy and Charley were the only storms that produced one EF-2 tornado.

It is important to note that no statistical verification of our scheme has yet been performed to quantify the ability of TCTP to forecast tornadoes. That will be the subject of future research. Nonetheless, our subjective analysis of a small sample of TCs leads us to believe that TCTP does have skill in assessing tornadic potential in landfalling TCs, particularly TCs of hurricane intensity.

Several modifications might improve the TCTP forecasts. First, developing separate regression equations for each quadrant of the storm could significantly strengthen the relationships between the component variables and tornadoes. We believe this could lead to a better quantification of tornadoes, particularly in the northeast quadrant. Another potential improvement would be to examine temperatures in the TC's core. Knowledge of the warm vs. cold core nature of the storm may enhance TCTP's forecast ability, particularly during times of extra-tropical transition. Finally, it would be desirable to expand the dataset to include storms whose centers are outside of our subset region since TCs sometimes continue to produce tornadoes days after landfall. With an adjustment or removal of the time term from landfall, TCTP forecasts could be extended to cover TCs for longer periods after landfall.

References

Baker, A. K., M. D. Parker, and M. D. Eastin, 2009: Environmental ingredients for supercells and tornadoes within Hurricane Ivan. *Wea. Forecasting*, **24**, 223–244.

Benjamin, S. G., K. J. Brundage, P. A. Miller, T. L. Smith, G. A. Grell, D. Kim, J. M. Brown, and T. W. Schlatter, 1994. The Rapid Update Cycle at NMC. Preprints, 10th Conf. Num. Wea. Pred., Portland, OR, July 18-22, 1994. Amer. Meteor. Soc., Boston, 566-568.

Benjamin, S. G. et al. 2002: NWS Technical Procedures Bulletin No. 490 RUC20 - The 20-km version of the Rapid Update Cycle.

Bogner, P. B., G. M. Barnes, and J. L. Franklin, 2000: Conditional instability and shear for six hurricanes over the Atlantic Ocean. *Wea. Forecasting*, **15**, 192–207.

Edwards, R., 2008: Tropical Cyclone Tornadoes -- A research and forecasting overview. Part 1: Climatologies, distribution and forecast concepts. http://spcwebsite.spc.noaa.gov/publications/edwards/hurr-sls.pdf, Preprints, 24th Conf. Severe Local Storms, Savannah GA.

Gentry, R. C., 1983: Genesis of tornadoes associated with hurricanes. *Mon. Wea. Rev*., **111**, 1793–1805.

Hill, E., W. Malkin, and J. W. A. Schulz, 1966: Tornadoes associated with cyclones of tropical origin-practical features. J. Appl. Meteor., **5**, 745–763.

Jarvinen, B. R., C. J. Neumann, and M. A. S. Davis, 1984: A tropical cyclone data tape for the North Atlantic basin, 1886-1983: Contents, limitations, and uses, *NOAA Technical Memorandum NWS NHC 22* (1984).

McCaul E. W. Jr., 1987: Observations of the Hurricane "Danny" tornado outbreak of 16 August 1985. *Mon. Wea. Rev*, **115**, 1206–1223.

McCaul E. W. Jr., 1991: Buoyancy and shear characteristics of hurricane tornado environments. *Mon. Wea. Rev*, **119**, 1954–1978.

McCaul E. W. Jr., and M. L. Weisman, 1996: Simulations of shallow supercell storms in landfalling hurricane environments. *Mon. Wea. Rev*, **124**, 408–429.

McCaul E. W. Jr., D. E. Buechler, S. J. Goodman, and M. Cammarata, 2004: Doppler radar and lightning network observations of a severe outbreak of tropical cyclone tornadoes. *Mon. Wea. Rev,* **132**, 1747-1763.

Novlan D. J., and W. M. Gray, 1974: Hurricane-spawned tornadoes. *Mon. Wea. Rev*, **102**, 476–488.

Pearson, A., and A. Sadowski, 1965: Hurricane-induced tornadoes and their distribution. *Mon. Wea. Rev*., **93**, 461–464.

Sadowski, A., 1962: Tornadoes associated with Hurricane Carla, 1961. *Mon. Wea. Rev*., **90**, 514–516.

Schultz, L. A. and D. J. Cecil, 2009: Tropical Cyclone Tornadoes, 1950-2007. *Mon. Wea. Rev.*, **137**, 3471–3484.

Smith, J. S., 1965: The hurricane-tornado. *Mon. Wea. Rev*., 93, 453–459.

Spratt S. M., D. W. Sharp, P. Welsh, A. Sandrik, F. Alsheimer, and C. Paxton, 1997: A WSR-88D assessment of tropical cyclone outer rainband tornadoes. *Wea. Forecasting*, **12**, 479–501.

Suzuki O., N. Hiroshi, O. Hisao, and N. Hiroshi, 2000: Tornado-producing mini supercells associated with Typhoon 9019. *Mon. Wea. Rev*, **128**, 1868–1882.

Verbout, D. Schultz, L. Leslie, H. Brooks, D. Karoly, and K. Elmore, 2007: Tornado outbreaks associated with landfalling hurricanes in the Atlantic basin: 1954–2004. *Meteor. Atmos. Phys*., **97**, 255–271.

Wilks, D.S., 2006. *Statistical Methods in the Atmospheric Sciences*, 2nd Ed. International Geophysics Series, Vol. 91, Academic Press, 627 pp.

FINAL REPORT OF THE SUBPROJECT ENTITLED:

"Vertical shear impacts on tropical disturbance development"

PAUL REASOR, PI
ELIZABETH MINTER, GRADUATE STUDENT

OUTLINE OF RESEARCH PROJECT

- Introduction
- Literature Review
  - Conditions and Mechanisms for Tropical Cyclogenesis
  - Tropical Disturbance Observations
  - Vertical Shear as a Hindrance to Disturbance Development
- Observational Motivation: Dolly (1996) and Claudette (2009)
- Numerical Model and Research Methodology
- Numerical Model Results
  - Control Experiment: Isolated Tropical Convection in a Quiescent Environment
  - Sensitivity Experiment 1: Isolated Tropical Convection in Uniform Horizontal Shear
  - Sensitivity Experiment 2: Isolated Tropical Convection in Vertical Shear
- Summary
- References

VERTICAL SHEAR IMPACTS ON TROPICAL DISTURBANCE DEVELOPMENT

II. Introduction

The transformation of a tropical disturbance characterized by persistent organized convection into a mature tropical cyclone with peak winds near the surface and a warm thermal anomaly in its core is the essence of tropical cyclogenesis. Tropical cyclogenesis is a complex process involving many interrelated processes on multiple spatial and temporal scales, ranging from the large-scale environment of the tropical disturbance to the individual convective towers within the disturbance. While the necessary large-scale conditions for tropical cyclogenesis have long been recognized, a large number of tropical disturbances in the tropical North Atlantic do not develop into mature tropical cyclones even when these large-scale conditions are met. *Forecasting such a complex transformation is difficult in itself; this forecasting challenge becomes especially problematic when the tropical disturbance is located near the coast. While such a system has little time to intensify, such rapid development leaves little time for coastal communities to prepare.*

This research subproject seeks to elucidate the mechanisms contributing to the observed sensitivity of the cyclogenesis process to vertical wind shear with the ultimate goal of improved understanding and forecasts of tropical cyclogenesis. With regards to the risk management issue, the representation of genesis in hurricane CAT models typically is performed by sampling the spatial distribution of genesis within the best-track dataset. As a consequence of this research, this sampling can take on a more physically detailed structure, by relating genesis on a finer scale to the known seasonal evolution of wind shear, and potentially capturing more unique genesis cases near the U.S. land mass where genesis is rarer but perhaps of greater threat given the decreased preparation time.

III. Literature Review

A. Conditions and Mechanisms for Tropical Cyclogenesis

The necessary conditions for tropical cyclogenesis are a layer of warm water, sufficient low-level instability to sustain deep convection, an upper-level environment supportive of sustained deep convection, and background rotation (e.g., Gray 1968). These large-scale conditions for tropical cyclogenesis are not sufficient to guarantee the formation of a mature tropical cyclone; a large number of tropical disturbances never develop into tropical cyclones in spite of favorable large-scale

conditions. Zehr (1992) determined from examination of infrared satellite imagery from a large number of developing and non-developing disturbances in the tropical West Pacific that developing tropical disturbances were accompanied by intense bursts of deep convection. These bursts of convection act to intensify the midlevel circulation of the tropical disturbance (Bister and Emanuel 1997; Simpson et al. 1997). Recent numerical work by Hendricks et al. (2004) and Montgomery et al. (2006) suggests that rapidly rotating deep convection also contributes directly to the spin-up of the low-level circulation. The convective updrafts amplify existing vorticity on the convective scale, which then grows upscale through vortex merger processes and is gathered by the system-scale convergence driven by heating within the convection.

B. Tropical Disturbance Observations

Multi-scale observations of the transformation of the tropical disturbance are limited due to the lack of observing systems over the ocean where tropical cyclogenesis occurs, but airborne dual-Doppler radar data (Reasor et al. 2005; Houze et al. 2009) and near-coastal Doppler radar (Sippel et al. 2006) provide evidence of strong rotation on convective scales within developing tropical disturbances.

C. Vertical Shear as a Hindrance to Disturbance Development

Idealized modeling studies of tropical cyclogenesis (e.g., Montgomery et al. 2006) have generally examined tropical cyclogenesis in ideal environments; the question usually is not whether genesis will occur for a given scenario, but whether the transformation of the initial disturbance occurs on a physically realistic timescale. Vertical wind shear is generally assumed to hinder genesis, as experience shows that such flows inhibit deep convection. Shear alone may be insufficient to prevent genesis, but may slow the transformation of the tropical disturbance to the point that other negative factors combine to prevent genesis. The role of vertical shear is far from simple, however; Reasor et al. (2004) demonstrated a dynamical mechanism by which tropical cyclone-scale vortices are resilient to weak to moderate vertical wind shear. It is unknown whether the same applies to intense cloud-scale vortices associated with rapidly rotating deep convection due to differences in scale, magnitude, and the close coupling of the vortex evolution to the convective evolution.

IV. Observational Motivation: Dolly (1996) and Claudette (2009)

Radar observations from two developing tropical disturbances were first analyzed to provide context for subsequent model results in terms of vorticity and convective structures in disturbance environments. The first case, Dolly (1996) was previously documented by Reasor et al. (2005). Here

the focus centers on the vertical structure of the vorticity and vertical motion fields relative to airborne Doppler-based local (10-100 km) and global analysis large-scale (100-1000 km) wind shear estimates. Claudette (2009) was not sampled extensively by airborne radar, but because of its development near land fell within range of multiple WSR-88D radars. Sippel et al. (2006) examined such a case with ground-based Doppler radar; they presented evidence of multiple interacting small-scale vortices associated with deep convection embedded within the larger-scale circulation. Fig. 3.1 from our analysis of Claudette shows small-scale velocity couplets in the vicinity of ongoing convection; these velocity couplets are indicative of convective-scale rotation. A more in-depth examination of the data will likely yield evidence of a significant number of these small-scale vortex signatures.

Figure 3.1.

Radial velocity at 1214Z on August 16, 2009, from the Tampa radar during the development of Tropical Storm Claudette.

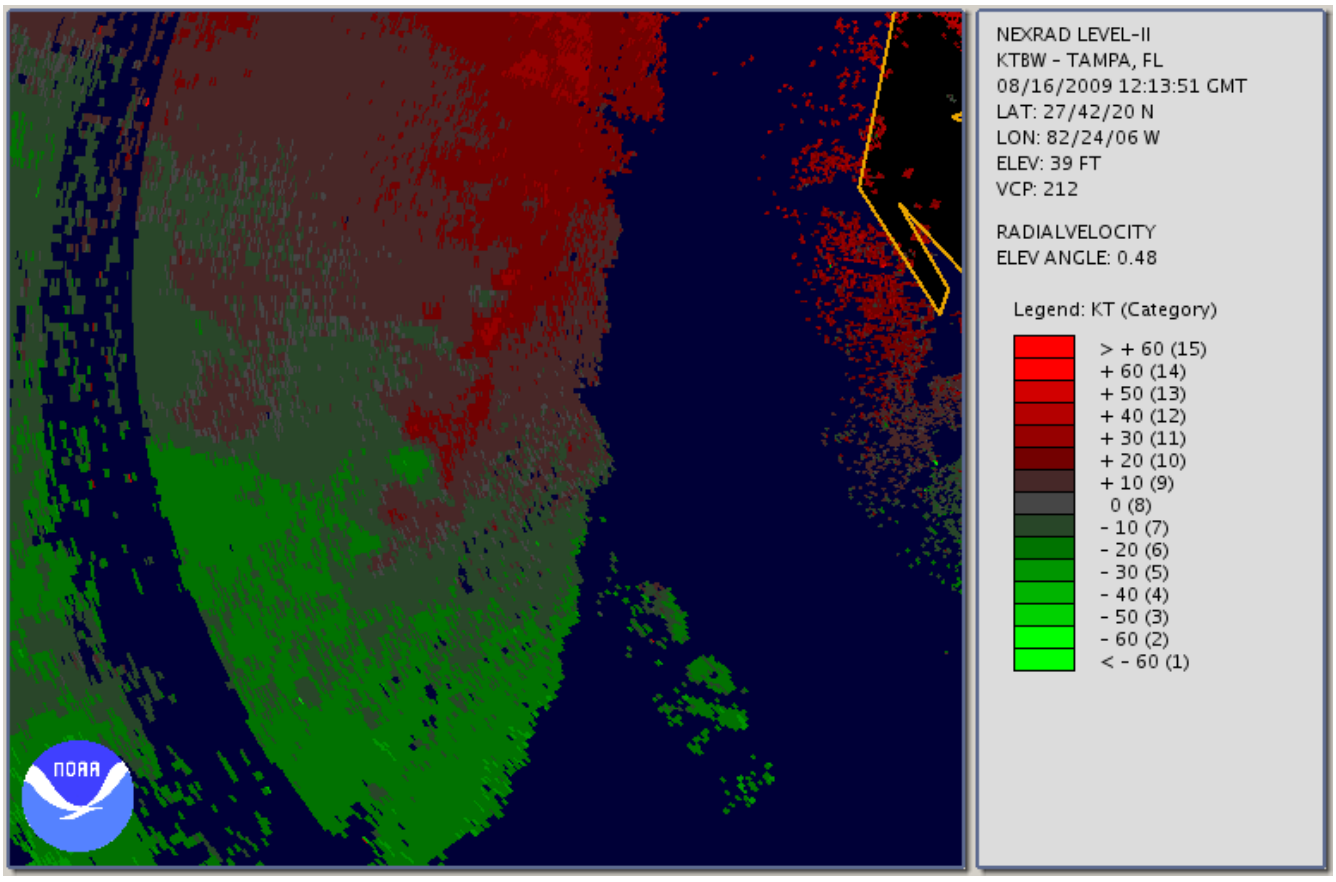

The genesis of Claudette caught forecasters by surprise; although the precursor disturbance was well-defined, and was first discussed by forecasters in the Tropical Weather Outlook 78 hours prior to the formation of the tropical depression, the forecast probability of development within 48 hours was

kept at less than 30% until just prior to the formation of the depression (Pasch 2010). It should be noted that near-coastal tropical cyclogenesis events like Claudette are not uncommon; between 1998 and 2007 there were 16 tropical cyclones that developed within 250 km of land – or approximately two per year. Depending on the subsequent track and speed, there may be little time for intensification to hurricane strength; however, there may be little time for coastal communities to prepare for the strong, gusty winds, heavy rain, and rough surf associated with weak tropical cyclones. For example, there was only 3 hours of lead time from the first tropical storm warning was issued until tropical storm-force winds were observed on the Texas coast during Tropical Storm Allison (2001); the associated tornadoes and flooding from heavy rain resulted in 41 deaths and an estimated $5 billion in damage (Stewart 2002). Fortunately, tropical Storm Claudette did not have such a drastic impact; despite less than 24 hours from the first tropical storm warning, there was only one death and minimal tree damage and sporadic power outages (Pasch 2010).

V. Numerical Model and Research Methodology

The difficulty in adequately measuring the structure and evolution of intense vortical convection during tropical cyclogenesis necessitates a numerical approach to understanding the factors influencing such development, and ultimately the genesis process. In order to examine the impact of vertical shear on rapidly rotating deep convection, cloud-resolving simulations were performed using the CM1 model (Bryan and Fritsch 2002), a full-physics three-dimensional cloud model. These simulations were run at order 100-meter resolution to examine the impact of vertical shear on tropical convection, both with and without background rotation. The convection was allowed to freely evolve from an initial heat bubble and develop vertical vorticity as part of its life cycle. These simulations were used to examine the structure and evolution of vertical vorticity, and the impact of vertical shear on the structure and life cycle of rotating tropical convection.

VI. Numerical Model Results

A. Control Experiment: Isolated Tropical Convection in a Quiescent Environment

The control run was performed with only planetary vorticity 3.77×10^{-5} s^{-1}; there was neither vertical shear nor background rotation. A bubble of heating 10km in radius horizontally and 2km radius vertically that produces a thermal anomaly of 2K over 5 minutes was used to initiate convection, with small-amplitude thermal anomalies to prevent resonance from wave reflection at the model boundaries. The subsequent evolution produced a nearly axisymmetric convective tower, with a classic convective

structure of a central updraft with surrounding downdrafts. Figure 3.2 shows the convective cell 30 minutes into the simulation. This convective cell developed strong cyclonic low-level vertical vorticity near the center surrounded by intense small-scale vortical features of both cyclonic and anticyclonic vorticity. Some of this vorticity is certainly due to the convergence of planetary vorticity; the fine-scale features are likely generated by the convective overturning of the convective cell.

Figure 3.2

Isosurface of reflectivity at 30 minutes in the control simulation.

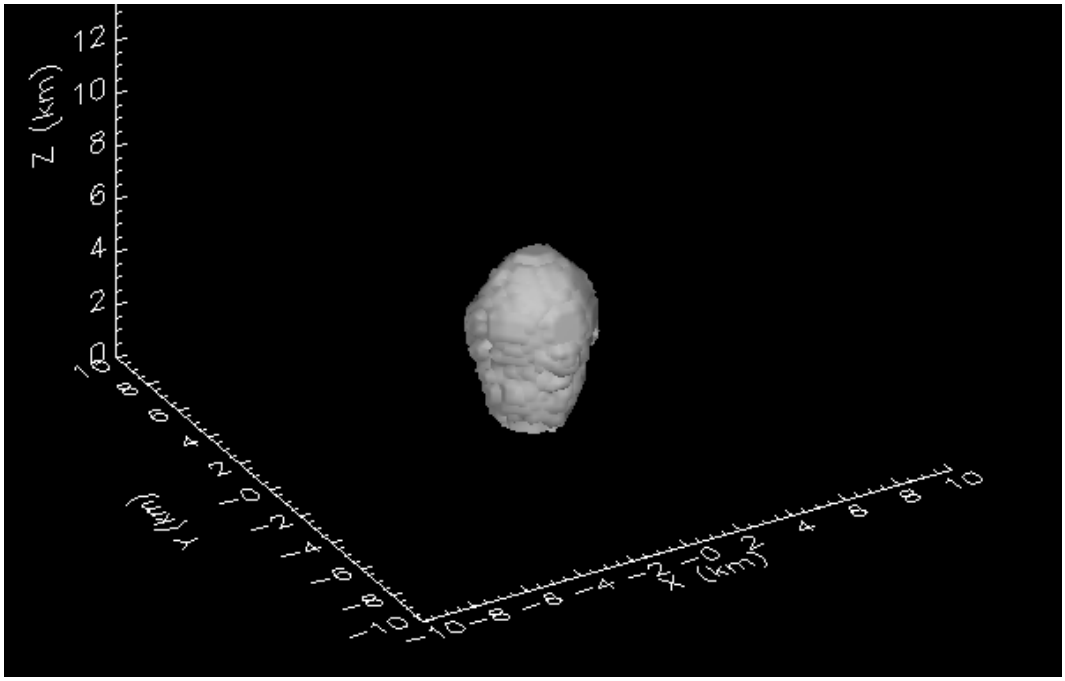

The radar data from Dolly (1996) suggests that these results are reasonable. The magnitude of the vorticity in the Dolly genesis environment is on the order of $1x10^{-5}$ s^{-1}; many of these vorticity features on scales of 10 km or less. Many of the stronger updrafts are located near some of the most intense vorticity features. There are also many strong vorticity features not associated with an updraft or downdraft; it is possible that these are remnants from earlier convection. Nonetheless, the detail and magnitude of the features in the simulation are in sufficient qualitative agreement that the use of high resolution, state of the art numerical modeling to pursue this problem is well-founded.

B. Sensitivity Experiment 1: Isolated Tropical Convection in Uniform Horizontal Shear

A horizontal straining flow of 10 m/s over 120 km with no vertical shear results in a background cyclonic relative vorticity of $8.3x10^{-5}$ s^{-1}, approximately 2 times the magnitude of the planetary vorticity. Convection evolving in such an environment initially develops an elliptical symmetry, as does

the associated vorticity; this symmetry is masked at later times by large-amplitude small-scale features generated by the turbulent motion of the convective overturning. The initial elliptical symmetry develops as a result of the horizontal strain on the developing cell induced by the background flow. At 25 minutes into the simulation, the magnitude of the vorticity averaged over 25km radius is roughly an order of magnitude larger for this case than for the control run. This result makes sense, since the background rotation provides additional vorticity beyond the planetary vorticity to be stretched by the convective updraft.

C. Sensitivity Experiment 2: Isolated Tropical Convection in Vertical Shear

A model run with 10 m/s of vertical shear through 20km depth and no background rotation except for planetary vorticity had a markedly different structure, both in the vorticity and overall convective fields. The vorticity initially develops couplets, with positive vorticity concentrated on one side of the shear vector and negative vorticity concentrated on the other side, although there were small-scale vorticity features of both signs on both sides of the shear vector. This is consistent with the tilting of shear-generated horizontal vorticity into the vertical by the convective updraft. Eventually, these small-scale features dominate the vorticity field, and the shear-induced wavenumber-1 asymmetry is no longer easy to pick out visually. There was a slight tilt to the convective tower; this downshear tilt is even more pronounced when the vertical shear is increased to 20 m/s (see Figure 3.3). At 25 minutes, the vertical vorticity averaged withing 25km radius of the center of the cell is roughly 7 times the magnitude of the vorticity in the control simulation; this increase in the average vorticity is likely due to the tilting of shear-generated horizontal vorticity into the vertical by the convective updraft.

Figure 3.3

Isosurface of reflectivity for the 20 m/s vertical shear simulation at 45 minutes.

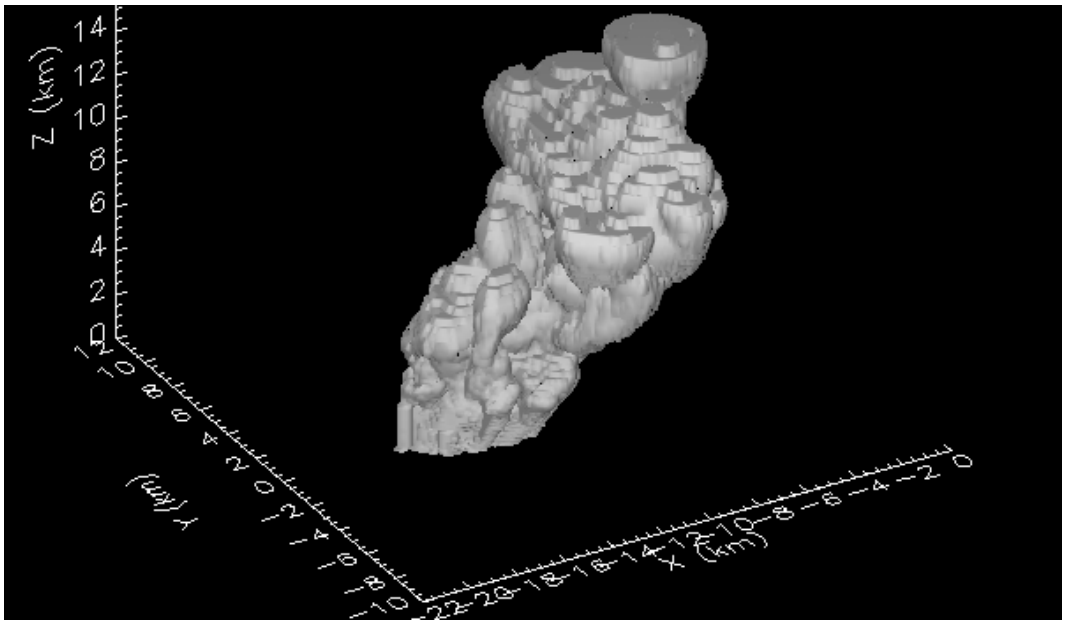

VII. Summary

The CM1 cloud-resolving model was configured to simulate tropical convection in idealized environments. Despite the idealized nature of the simulations, the results thus far compare well with prior numerical simulations of deep convection. As expected, the presence of background rotation contributed to larger amplitudes of vorticity in the simulated convective cells. The presence of vertical wind shear was not detrimental to the development of convective-scale rotation; the tilting of shear-generated horizontal vorticity into the vertical by the updraft resulted in an enhancement of the vorticity generated by convergence of planetary vorticity.

In order to draw further conclusions about the impact of vertical shear on the structure and evolution of rotating deep convection, several further model simulations need to be conducted, some with stronger background rotation and others with both background rotation and vertical shear. A few simulations will also need to be conducted with weaker and stronger convective instability in order to determine how the impact of the vertical shear and the background rotation is related to instability. The model simulations currently only extend 1 hour of model time; it is necessary to extend the time further to determine both the impact of the vertical shear and background rotation on the lifetime of the convective cells as well as to determine how long the vorticity generated by a convective tower persists as a coherent feature once the convective cell dies away.

In these simulations, the presence of vertical shear did not inhibit the development of vortical convection, but rather provided an additional source of vorticity through generation of horizontal

vorticity that can be tilted into the vertical by convective updrafts. However, these simulations have been conducted in an idealized tropical disturbance environment with a horizontally uniform background thermal profile; it is possible that the total impact of vertical shear on tropical cyclogenesis is a balance between the enhancement of convective-scale vorticity seen in these simulations and the inhibition of convection inherent in bringing drier, more stable air into the tropical disturbance. This would complicate genesis forecasting somewhat, as vertical shear is generally considered to be detrimental to tropical cyclogenesis. However, before such complex impacts of vertical shear can be accounted for in forecasting genesis, the impact of convective-scale rotation would also have to be included. Through additional simulations and sensitivity experiments it is hoped that the predictability of TC genesis can be further refined, including identifying regimes in which genesis predictability is enhanced or suppressed due to the large scale environment.

REFERENCES

Bister, M., and K. A. Emanuel, 1997: The genesis of Hurricane Guillermo: TEXMEX analyses and a modeling study. *Mon. Wea. Rev.*,**125**, 2662–2682.

Bryan, G. H., and J. M. Fritsch, 2002: A benchmark simulation for moist nonhydrostatic numerical models. *Mon. Wea. Rev.*, **130**, 2917–2928.

Gray, W. M., 1968: Global view of the origin of tropical disturbances and storms. *Mon. Wea. Rev.*, **96**, 669 – 700.

Hendricks, E. A., M. T. Montgomery, and C. A. Davis, 2004: The role of ``vortical" hot towers in the formation of tropical cyclone Diana (1984). *J. Atmos. Sci.*,**61**, 1209–1232.

Houze, R. A., W-C Lee, and M. M. Bell, 2009: Convective contribution to the genesis of Hurricane Ophelia (2005). *Mon. Wea. Rev.*, **137**, 2778-2800.

Montgomery, M. T., M. E. Nicholls, T. A. Cram, and A. B. Saunders, 2006: A vortical hot tower route to tropical cyclogenesis. *J. Atmos. Sci.,* **63**, 355–386.

Pasch, R. J, 2010: Tropical cyclone report: Tropical Storm Claudette 16 – 17 August 2009. National Hurricane Center Rep., 8p. [Available online at http://www.nhc.noaa.gov/2009atlan.shtml].

Reasor, P. D., M. T. Montgomery, and L. F. Bosart, 2005: Mesoscale observations of the genesis of Hurricane Dolly (1996). *J. Atmos. Sci.,* **62**, 3151–3171.

Reasor, P. D., M. T. Montgomery, and L. D. Grasso, 2004: A new look at the problem of tropical cyclones in vertical shear: Vortex resiliency. *J. Atmos. Sci.*, **61**, 3–22.

Simpson, J, E. Ritchie, G. J. Holland, J. Halverson, and S. Stewart, 1997: Mesoscale interactions in tropical cyclone genesis. *Mon. Wea. Rev.*, **125**, 2643 – 2661.

Sippel, J. A., J. W. Nielsen-Gammon, and S. E. Allen, 2006: The multiple-vortex nature of tropical

cyclogenesis. *Mon. Wea. Rev.,* **134**, 1796–1814.

Stewart, S. R., 2002: Tropical cyclone report: Tropical Storm Gert 5 – 17 June 2001. National Hurricane Center Rep.[Available online at http://www.nhc.noaa.gov/2001atlan.shtml].

Zehr, R. M., 1992: Tropical cyclogenesis in the western North Pacific. NOAA Tech. Rep. NESDIS 61, U.S. Department of Commerce, Washington, DC 20233, 181 pp.